JAERI-M
9765

THROUGH ANALYSIS OF LOFT L2-3 BY THYDE-P CODE

(SAMPLE CALCULATION RUN 40)

October 1981

Masashi HIRANO

日本原子力研究所
Japan Atomic Energy Research Institute

この報告書は，日本原子力研究所がJAERI-Mレポートとして，不定期に刊行している研究報告書です．入手，複製などのお問合わせは，日本原子力研究所技術情報部（茨城県那珂郡東海村）あて，お申しこしください．

JAERI-M reports, issued irregularly, describe the results of research works carried out in JAERI. Inquiries about the availability of reports and their reproduction should be addressed to Division of Technical Information, Japan Atomic Energy Research Institute, Tokai-mura, Naka-gun, Ibaraki-ken, Japan.

JAERI-M 9765

Through Analysis of LOFT L2-3 by THYDE-P Code

(Sample Calculation Run 40)

Masashi HIRANO

Division of Reactor Safety Evaluation
Tokai Research Establishment, JAERI

(Received October 1, 1981)

A through calculation of Experiment L2-3 of the Loss-of-Fluid Test (LOFT) Facility Power Ascension Series (Experiment Series L2) was performed with the THYDE-P code. The specific objectives of Experiment L2-3 were to determine the thermal-hydraulic behavior of the nuclear core and the thermal-mechanical response of the fuel rod cladding with a maximum linear heat generation rate of 39.4 kW/m. The THYDE-P code is a computer code to analyze both the blowdown and refill-reflood phases of loss-of-coolant accidents (LOCAs) of pressurized water reactors (PWRs) without a change in the methods and the models and is now under verification study and modification. The present calculation was performed by best estimate (BE) options as Sample Calculation Run 40, which is a portion of a series of THYDE-P sample calcultions. The calculation was carried out from test initiation until complete submersion of the core volume with subcooled water, i.e. about 60 sec. The trend of the calculated cladding surface temperature was in good agreement with that of the experimental results.

Keywords : LOFT, LOCA, PWR, THYDE-P Code, Verification Study, Sample Calculation, Fuel Rod Cladding, Blowdown, Reflood

JAERI-M 9765

THYDE－PコードによるLOFT　L２－３の一貫解析

（サンプル計算Run 40）

日本原子力研究所東海研究所安全解析部

平野　雅司

（1981年10月1日受理）

LOFT計画における出力上昇実験シリーズ（シリーズL２）中の実験L２－３の一貫解析を，THYDE－Pコードを用いて行った。L２－３実験の目的は，最大線出力密度39.4 kW/mにおける炉心の熱水力学的挙動，および燃料被覆管の熱機械学的挙動を同定することにあった。THYDE－Pコードは，加圧水型軽水炉の冷却材喪失事故のブローダウン，および再冠水過程を，手法やモデルの変更なしに一貫して解析する計算コードであり，現在，検証計算，および修正を行っている。本解析は最適評価オプションを用い，サンプル計算Run 40として行ったものであり，一連のTHYDE－Pサンプル計算の一部を成すものである。計算は，実験開始後炉心が完全に未飽和水下に没するまで（約60秒）行った。計算された燃料被覆管表面温のふるまいは，実験値との良い一致を示した。

目　　次

CONTENTS

LIST OF FIGURES

LIST OF TABLES

1. Introduction

A through calculation of LOFT L2-3[1][2] was performed with the THYDE-P code[3][4][5] not only to verify the system performance of THYDE-P but also to obtain better understanding of the experiment.

Experiment L2-3 was the second test in the Power Ascension Series (Experiment Series L2) of nuclear double-ended cold leg break tests and conducted at a maximum linear heat generation rate of 39.4 kW/m (36.7 MW). This power level is about 75% of the LOFT rated thermal power level of 50 MW and corresponds to the nominal full power operation of a commercial PWR. The LOFT ECCS simulates the ECCS of a commercial PWR. The accumulator (ACC), the high-pressure injection system (HPIS), and the low-pressure injection system (LPIS) were used during the experiment. Each system was arranged to inject scaled flow rates into the primary coolant system cold leg. Electrical power to the primary system motor generator sets was terminated 200 sec. after blowdown initiation and the primary coolant pumps began to coast down. The core volume reflood time was about 55 sec. after rupture[1].

In the present analysis, the LOFT system was nodalized into 43 nodes and 37 junctions. The active core was simulated by 4 nodes. A hot channel analysis was not performed but only an average channel analysis was done. The discharge coefficient for the Moody correlation[7] was set to be 0.8. The ACC water temperature was given by an input as 307 °k, which was the same as the experimental data. In order to avoid unrealistically large pressure decrease due to low enthalpy ECC water, a time delay model[4] for density change, which takes non-equilibrium effects into consideration, was applied.

The calculation proceeded until the core nodes were completely submerged with subcooled water, i.e. about 60 sec. after rupture, without any calculation mode change during the entire process. At the early stage of the blowdown phase, one or two peakes of the cladding surface temperture were also calculated as were observed in the experiment.

2. Description of LOFT L2-3

2.1 Primary Objectives

The specific objectives of Experiment L2-3 were to determine the thermal-hydraulic behavier of the nuclear core and the thermal-mechanical response of the fuel rod cladding with a maximum linear heat generation rate of 39.4 kW/m. The LOFT facility was configured to simulate a postulated loss-of-coolant accident in a commercial pressurized water reactor (~1000 MWe) resulting from a 200% double-ended offset shear break in the cold leg of the primary coolant system. During system depressurization into a simulated containment, emergency core cooling water was injected into the primary coolant system cold leg to provide data on the effects of emergency core cooling on system thermal-hydraulic response.

2.2 System configuration and Experiment Procedures

The LOFT major components are shown in Fig. 2.1. The core contains 1300 nuclear fuel rods arranged in five square and four triangular (corner) fuel modules, shown in Figure 2.2. On the detailed information on the LOFT system configuration, reference shoud be made to Ref. (1) and (2).

Immediately prior to blowdown, the pressurizer heaters were turned off. The quick-opening blowdown valve-2 (QOBV-2) commenced opening 1.9 msec before QOBV-1 and opened to the flow area of a 12-inch Schedule 60 (0.3 mm OD) pipe in 19.1 msec; QOBV-1 opened to the same flow area in 17.2 msec. Electrical power to the primary system motor generator sets was terminated at 200 sec after blowdown initiation. Emergency coolant injection was directed to the intact loop cold leg during blowdown. Injection from accumulator ACC-A at a system pressure of 4.18 MPa began approximately 17 sec after initiation of blowdown and continued for 32 sec. The HPIS flow was initiated by LOCE control 14 sec after the initiation of blowdown and was injected 1.3 l/sec. The LPIS flow was initiated by LOCE control 29 sec after the initiation of blowdown. Nitrogen gas from the accumulator entered the system at 49 sec and continued to flow for about 11 sec.

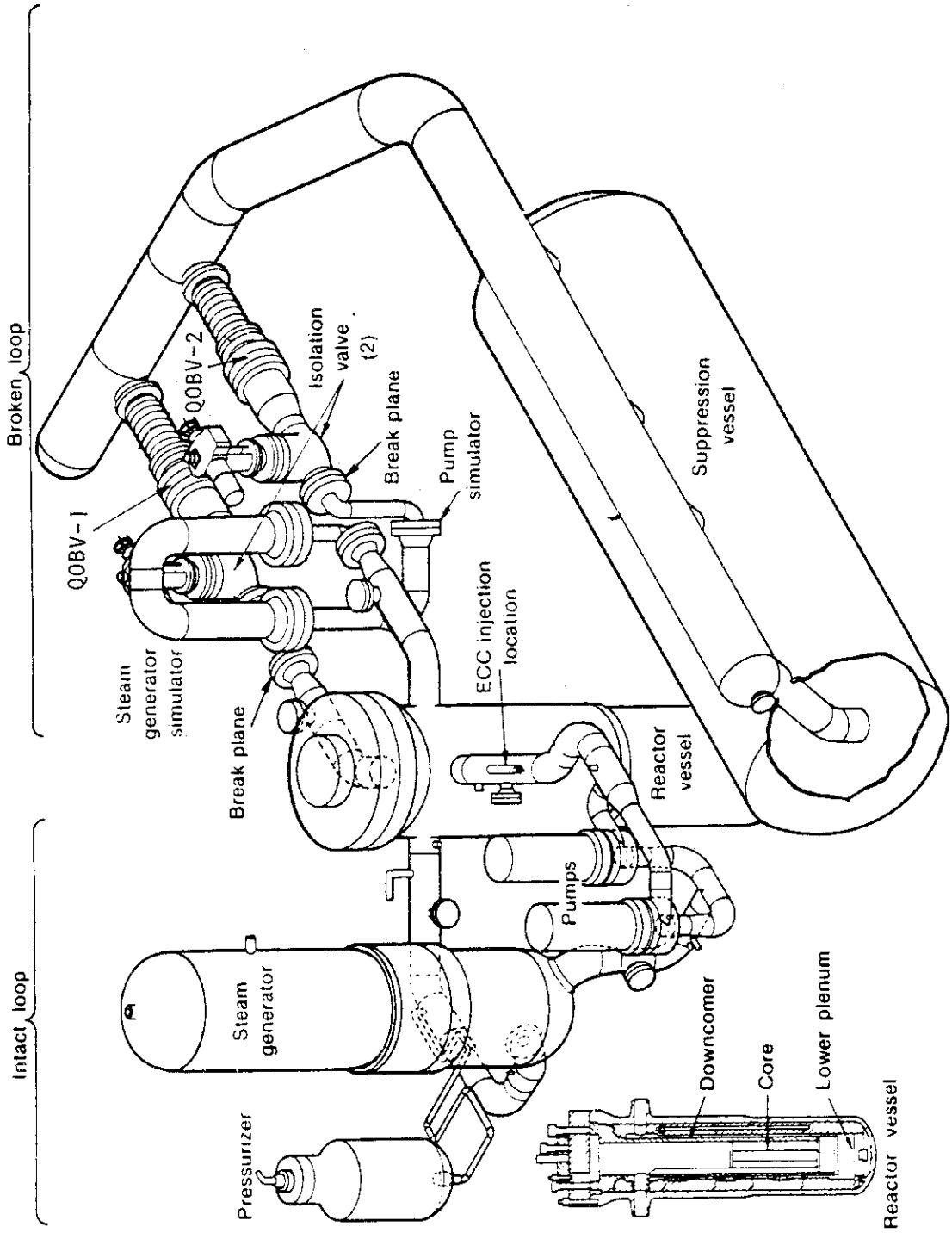

Fig. 2.1 LOFT Major Components

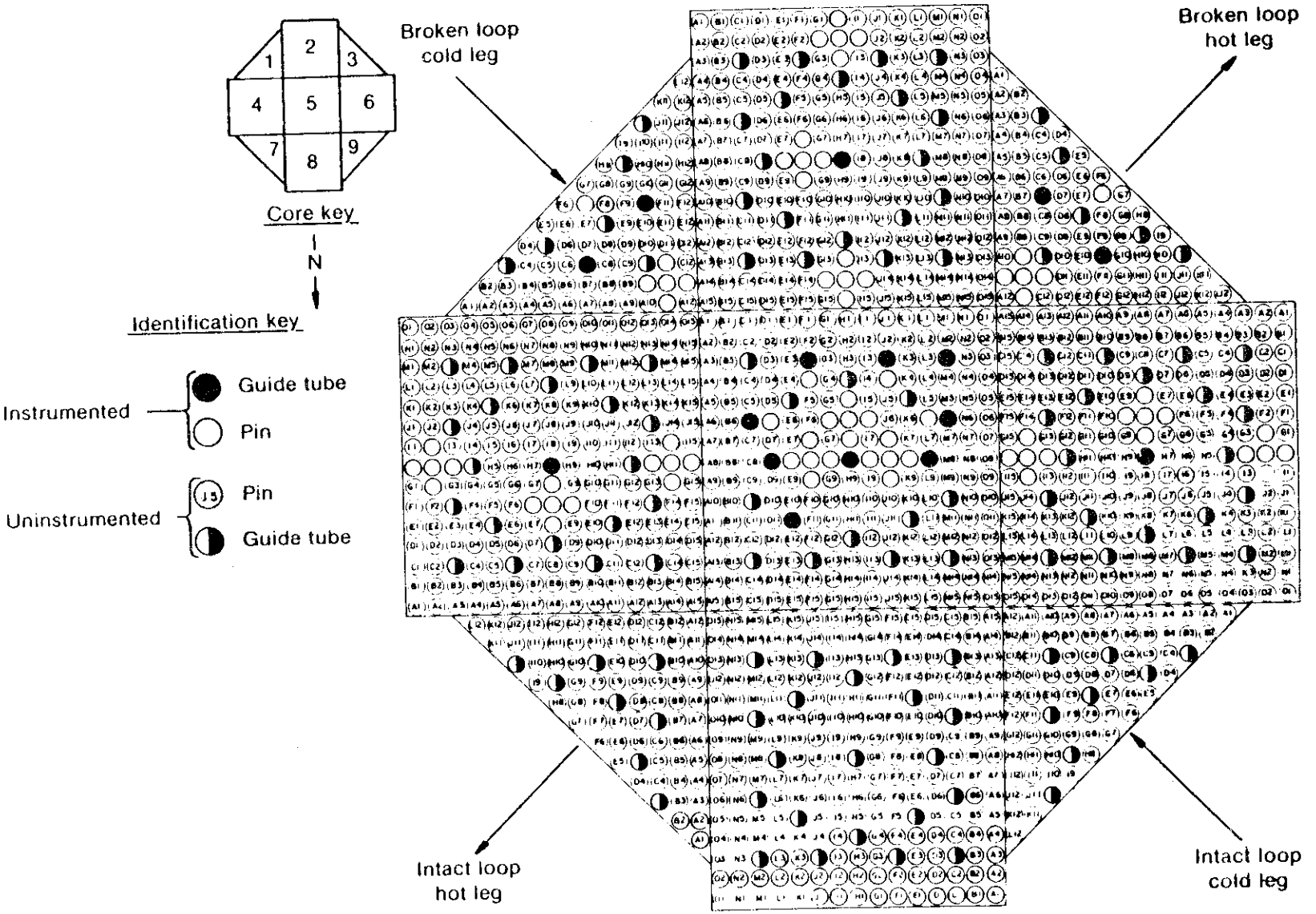

Fig. 2.2 LOFT Core 1 Configuration Showing Rod Designation

3. Analytical Models in Present Calculation

The models and the methods of the THYDE-P code are presented in detail in Ref. (3), some of which have been revised[4][5]. Several models which may be most relevant to the present analysis are briefly descrived in this section.

3.1 CHF Correlations

In the present calculation, the Biasi correlation[13] and the modified Zuber correlation[16][17] were adopted to predict CHF values for $G > G_{min}$ and $G \leq G_{min}$, respectively, where G_{min} = 273 kg/m^{2}s.

3.2 Heat Transfer Correlations

The heat transfer correlations tentatively applied in the present calculation are listed in Table 3.1.1 and 3.1.2 In heat transfer mode 4-5 (pool transition boiling), it was assumed that the Berenson correlation[19] was not applicable when coolant quality was small enough, i.e. less than x_c. For simplicity in the present calculation, the heat flux value was set to be a constant ϕ_c. Namely,

$$\phi = \phi_c \quad \text{when} \quad x < x_c$$

where

x_c = 0.1

ϕ_c = 50 kcal/m^{2}s (64,000 Btu/ft^{2}s) .

This heat transfer mode 4-5 played an important role in the reflooding calculation as will be shown in Sec. 5.

3.3 Break Flow Calculation

The slightly modified[3] Zaloudek correlation[6] and the Moody correlation[7] are implemented for a subcooled and a saturated condition, respectively, in the present version of THYDE-P. The discharge coefficient for the Moody correlation was assumed to be 0.8, which was the same as that in the analysis of LOFT L2-2[4].

Table 3.1.1 Heat Transfer Correlations

Mode		Conditions		Correlations
Core	SG	Coolant Condition	Other conditions	
1	1	Subcooled water	$T_{wall} < T_{sat}$	Dittus-Boelter[9]
2	2	Subcooled water	$T_{wall} > T_{sat}$	Interpolation between D-B and J-L
3	3	Saturated state	$\phi < \phi_{CHF}$	Jens and Lottes[10]
4	/	Saturated state	$\phi > \phi_{CHF}$	(see Table 3.1.2)
5	5	Superheated steam	$Re < 3000$	McEligot[12]
6	6	Superheated steam	$3000 < Re < 5000$	McEligot[12]
7	7	Superheated steam	$Re > 5000$	McEligot[12]
/	8	Saturated state	$T_{coolant} > T_{wall}$	Condensation[14]

Table 3.1.2 Heat Transfer Correlations in Mode 4

Mode	Conditions	Correlations
4-1	$G > Gmin$, $\phi_{4-1} > \phi_{4-2}$	McDonough, Milich and King[15]
4-2	$G > Gmin$, $\phi_{4-1} < \phi_{4-2}$	Groenevelt[11]
4-3	$G < Gmin$, $\Delta T_s < \Delta T_{min}$	Pool transition boiling correlation[8]
4-4	$G < Gmin$, $\Delta T_s > \Delta T_{min}$	Berenson[19]
4-5	$G < Gmin$, $x < x_c$	Pool transition boiling

3.4 Time Delay Model for Density Change

It is well known that thermal non-equilibrium effects due to low enthalpy ECC water injection is considerably large. In general in analyses by thermal equilibrium models, calculations may fail beacuse of unrealistically large pressure drop due to an overestimated condensation rate. In THYDE-P, to avoid the difficulty, a time delay model for density change[4] which takes into account phenomenologically non-equilibrium effects is implemented as follows:

$$\frac{\partial \rho^*}{\partial t} = \frac{\rho - \rho^*}{\tau_D} \qquad (3.4.1)$$

where

$$\rho^* = \alpha^* \rho_{gs} + (1-\alpha^*)\rho_{fs}$$

$$\rho = \alpha \rho_{gs} + (1-\alpha)\rho_{fs}$$

and

ρ equilibrium node average density

ρ^* non-equilibrium node average density

α equilibrium void fraction

α^* non-equilibrium void fraction.

The parameter τ_D in Eq. (3.4.1) is called a delay parameter which specifies the time delay of the average density. It should be noted that when τ_D asymptotically approches to zero, the model reduces to the equilibrium model, i.e. $\rho^* = \rho$. In the present analysis, this model was applied after ACC injection initiated. In the model, what is the most difficult is to determine the delay parameter, which may be dependent on flow regimes, node geometries, pressure, etc. In the present analysis, a simple formulation, which is the same as that in the analysis of LOFT L2-2[4], was assumed as follows:

$$\tau_D = \begin{cases} 0 & x > x_0 \\ c_n\{\cos(x/x_0) + 1\}/2 & 0 < x < x_0 \\ c_n & x < 0 \end{cases} \qquad (3.4.2)$$

where

$x = (h - h_{fs})/h_{gs}$, and

$x_0 = 0.2$

and the constant c_n is so given as to be proportional to the node volume with c_n = 1 sec for the core nodes. This formulation for τ_D is the same as that tentatively applied in the analysis of LOFT L2-2[4]. A physical model to evaluate the parameter is yet to be developed.

4. Input Data and Results of Steady State Adjustment

The input data in the present analysis are listed in App. A. The initial conditions are compared with the experimental data in Table 4.1. The input data and the results of steady state adjustment[3] are summarized in this section.

(1) Nodalization

The nodalization scheme in the present analysis is shown in Figs. 4.1 (a) and (b) and the node geometrical data are shown in Table 4.2. The pressure vessel is expressed by nodes from 22 to 33. The downcomer was simulated by a single node whose number was 22. The active core was nodalized into 4 nodes, i.e. nodes from 26 to 29. The double-ended break was assumed to occur at junction 6. ECC water was injected into mixing junction 26.

The loss coefficients of nodes are listed in Table 4.3.

(2) Trip Data

The following trip actions were taken by inputs as follows.

Trip action	Time after rupture (s)
SG secondary feed water stop	0.002
SCRAM	0.103
HPIS injection initiation	14.0
LPIS injection initiation	29.0

(3) Core Data

Initial power level 36 MW .

The initial heat fluxes are shown as follows.

Node No.	Heat flux (kcal/m^{2}s)
25	106.6
26	179.7
27	137.0
28	45.4

Number of fuel rods	1300
Cladding outer diameter	1.072×10^{-2} m
Cladding thickness	6.172×10^{-4} m
Fuel pelet diameter	8.934×10^{-3} m
Rod pitch	1.430×10^{-2} m
Gap gas mole number	0.57 mole
Plenum gas volume	5.493×10^{-6} m^3

The gas molecular fractions of the gap gas are listed as follows.

Gas	Molecular fraction (-)
He	0.887
Xe	0.0355
Kr	0.0063
N_2	0.0712

As a result of steady state adjustment, the following properties were obtained.

Steady state gap pressure 3.0×10^5 Pa .

The fuel center temperatures, the cladding surface temperatures and the heat transfer coefficients are shown as follows.

Node No.	Fuel ceter temp.(°c)	Cladding surface temp.(°c)
24	287.9	287.9
25	782.8	325.1
26	1173.8	346.0
27	950.6	346.0
28	518.1	333.0
29	320.9	320.9

Node No.	Heat transfer coefficient ($kcal/m^2 s°c$)	
	Cladding surface	Gap
25	3.64	0.51
26	4.76	0.56
27	4.88	0.53
28	3.77	0.48

(4) Steam Generator Data

The primary and secondary systems of the steam generator were simulated by nodes 13 to 16 and node 42, respectively. Nodes 14 and 15 simulated primary coolant in the U-tubes. The input data for the steam generator are summarized as follows.

Plenums	
Volume	0.353 m^3
Hydraulic diameter	0.908 m
Height	0.518 m
U-tubes	
Number	1845
Outer diameter	1.021×10^{-2} m
Height	2.483 m
Pitch	1.905×10^{-2} m
Secondary system	
Pressure	60.99 atm
Feed water enthalpy	213.8 kcal/kg
Feed water mass flow rate	19.5 kg/s
Flow area	1.589 m^2
Height	4.188 m
Subcooled water level	0.3 m
Void fraction of saturated region	0.3

The initial heat flux values are listed as follows.

Node No.	Heat flux ratio (-)
13	0.71
14	0.29

The results of steady state adjustment concerning the steam generator are listed as follows.

Region	Enthalpy (kcal/kg)	Bulk temperature (°c)	Mass (kg)
Saturated	298.8	277.4	3324.
Subcooled	213.8	209.4	408.5

Node No.	Wall temperature (°c)	
	Primary side	Secondary side
14	560.2	554.9
15	556.7	551.8

Node No.	Hear transfer coefficient ($kcal/m^2s°c$)	
	Primary side	Secondary side
14	3.90	7.87
15	3.85	4.65

(5) Pressurizer Data

The input data for the pressurizer, node 41, are summarized as follows.

Flow area	0.557 m^2
Height	1.7235 m
Subcooled water level	0.4 m
Void fraction of saturated region	0.4 .

The results of steady state adjustment were as follows:

Steady state pressure	15.07 MPa
Enthalpy of saturated region	408.8 kcal/kg
Enthalpy of subcooled region	346.6 kcal/kg
Total mass of saturated region	294.9 kg
Total mass of subcooled region	151.3 kg .

(6) Pump Data

The primary coolant pumps were simulated by nodes 18 and 19.

Rated speed	3530 rpm
Rated flow	0.3155 m^3/s
Rated head	108.1 m
Rated torque	500.24 J/rad
Rated density	613.73 kg/m^3

Moment of inertia	1.4382 kg m^2/rad^2
Steady state speed	1270 rpm

In the present analysis, the constant pump speed option was applied throughout the analysis. As to the single-phase and two-phase pump characteristic curves, reference should be made to Ref. (4).

(7) ECCS Data

Accumulator

Liquid volume	1.71 m^3
Gas volume	0.96 m^3
Liquid enthalpy	34.2 kcal/kg
Initial pressure	41.25 atm

The total liquid mass was calculated to be 1.703×10^3 kg.

HPIS and LPIS

Liquid enthalpy	24 kcal/kg

The injection mass flow rates from HPIS and LPIS were given by inputs as time tables based on the experimental data.

(8) Simulated SG and Pump Data

The simulated SG and pump in the broken loop hot leg were nodalized into nodes 3 to 7. The loss coefficients in these nodes are shown in Table 4.3.

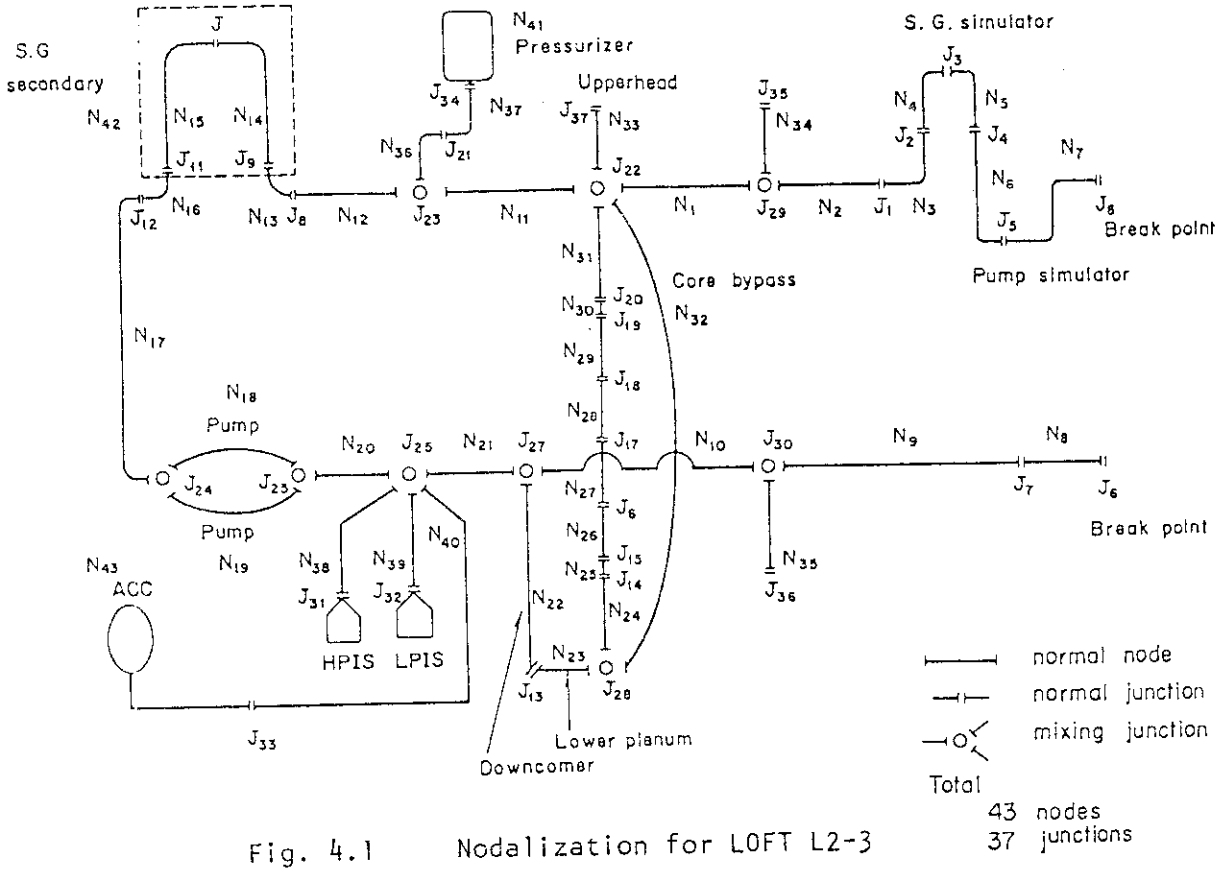

Fig. 4.1 Nodalization for LOFT L2-3

(a) Major components

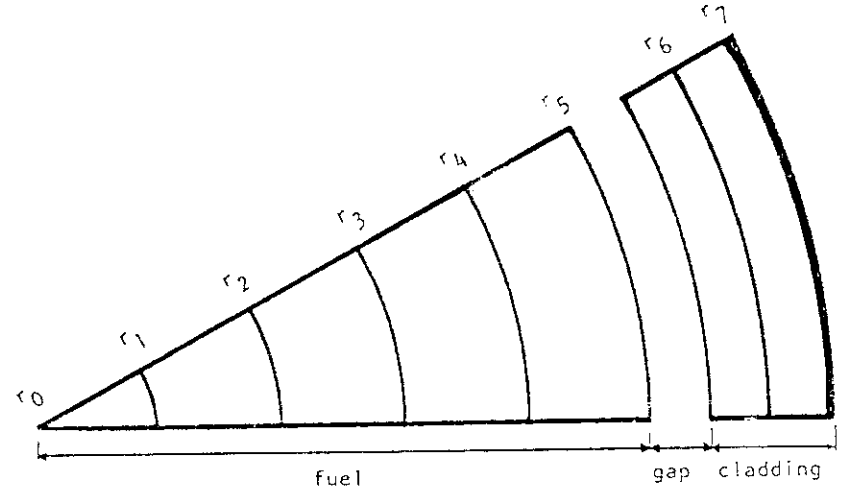

Fig. 4.1 Nordalization for LOFT L2-3

(b) Within fuel rod

Table 4.1 Initial Conditions for LOFT L2-3

Items	Measured value	Analysis
Primary coolant system		
Mass flow rate (kg/s)	199±6.3	199.0
Pressure (MPa)	15.06±0.03	15.08
Cold leg temperature (K)	560.7±1.8	561
Hot leg temperature (K)	592.9±1.8	593
Reactor vessel		
Power level (MW)	36±1	36.0
Maximum linear heat generation rate (kW/m)	39±3	22.4
Pressurizer		
Steam volume (m^3)	0.293±0.008	0.295
Water volume (m^3)	0.670±0.008	0.665
Water temperature (K)	615.3±3.0	613(a), 593(b)
Pressure (MPa)	15.06±0.03	15.07
Level (m)	1.19±0.01	1.19(c)
Broken loop		
Hot leg temperature (K)		
Near vessel	565.5±1.8	593
Near break	556.5±1.8	593
Cold leg temperature (K)		
Near vessel	554.3±1.8	561
Near break	550.3±1.8	561
Steam generator secondary side		
Water level (m)	3.11±0.025	3.02(c)
Water temperature (K)	482.1±3	550(a), 482(b)
Pressure (MPa)	6.18±0.08	6.18
Mass flow rate (kg/s)	19.5±0.4	19.5
Accumulator		
Gas volume (m^3)	0.96±0.03	0.96
Water volume injected (m^3)	1.71±0.03	1.71
Temperature (K)	307.2±3	307

(a) and (b) indicate saturated region and subcooled region, respectively.
(c) : What is called "collapsed water level".

Table 4.2 Node Geometrical Data

Node No.	Description	Flow Area A (m^2)	Node Length L (m)	Node Height H_L (m)
1	Broken loop hot leg	0.06344	1.332	0.0
2	Broken loop hot leg	0.06344	0.6965	0.0
3	Broken loop hot leg	0.00836	1.517	0.7174
4	Broken loop hot leg	0.09539	3.228	2.705
5	Broken loop hot leg	0.09539	3.228	-2.705
6	Broken loop hot leg	0.01271	2.423	-2.039
7	Broken loop hot leg	0.008365	1.883	1.322
8	Broken loop cold leg	0.008365	0.4877	0.0
9	Broken loop cold leg	0.06344	0.6965	0.0
10	Broken loop cold leg	0.06344	0.9510	0.0
11	Intact loop hot leg	0.06344	2.6160	0.0
12	Intact loop hot leg	0.06299	2.643	0.2423
13	SG inlet plenum	0.6481	0.5175	0.5175
14	SG U-tube	8.187 E-5	2.568	2.483
15	SG U-tube	8.187 E-5	2.568	-2.483
16	SG outlet plenum	0.6481	0.5175	-0.5175
17	Crossover leg	0.06793	2.429	-1.523
18	Pump	0.09446	1.867	1.281
19	Pump	0.07273	3.111	1.281
20	Intact loop cold leg	0.0597	1.399	0.0
21	Intact loop cold leg	0.06343	0.5313	0.0
22	Downcomer	0.1604	4.256	-4.256
23	Lower plenum	0.7917	0.7318	0.0
24	Mixing box	0.1532	0.4285	0.4285
25	Active core	1.143 E-4	0.09423	0.09423
26	Active core	1.143 E-4	0.4191	0.4191
27	Active core	1.143 E-4	0.4191	0.4191
28	Active core	1.143 E-4	0.4191	0.4191
29	Active core	1.143 E-4	0.4191	0.4191
30	Active core	1.143 E-4	0.01753	0.01753
31	Upper core structures	0.2387	1.668	1.668

(continued)

32	Core bypass	4.766 E-3	4.146	4.146
33	Upper head	0.2306	0.9144	0.9144
34	Reflood assist line	0.03871	4.048	0.8620
35	Reflood assist line	0.03871	4.840	0.6075
36	Pressurizer surge line	1.452 E-3	4.592	0.4255
37	Pressurizer surge line	1.452 E-3	4.767	0.7678
38	ECCS piping	6.221 E-3	5.5	0.0
39	ECCS piping	6.221 E-3	5.5	0.0
40	ECCS piping	6.221 E-3	58.0	0.0

Table 4.3 Loss Coefficients of Nodes

Node No.	k	k^{Af}	k^{Ar}	k^{Ef}	k^{Er}
1	0.022	0.4	0.8	0.0	0.0
2	0.020	0.0	0.0	0.0	0.0
3	0.019	0.39	0.75	1.52	1.09
4	0.030	0.0	0.0	189.	189.
5	0.016	0.0	0.0	142.	198.
6	0.019	0.0	0.0	20.	20.
7	0.017	0.0	0.0	-	-
8	0.019	-	-	0.754	0.391
9	0.029	0.0	0.0	0.0	0.0
10	0.017	0.0	0.0	3.58	3.58
11	0.020	0.4	0.8	0.0	0.0
12	0.027	0.0	0.0	0.815	0.815
13	0.026	0.0	0.0	0.0	0.0
14	0.0	0.345	0.588	0.0	0.0
15	0.0	0.0	0.0	0.588	0.345
16	0.029	0.0	0.0	0.0	0.0
17	0.020	0.403	0.801	0.0	0.0
18	0.117	0.0	0.0	0.0	0.0
19	0.021	0.0	0.0	0.0	0.0
20	0.017	0.0	0.0	0.0	0.0
21	0.020	0.0	0.0	3.58	3.0
22	0.013	0.62	0.62	3.5	3.5
23	0.014	0.0	0.0	0.0	0.0
24	6.58	0.0	0.0	0.0	0.0
25	3.11	0.014	0.0	0.0	0.0
26	3.12	0.0	0.0	0.0	0.0
27	3.24	0.0	0.0	0.0	0.0
28	2.92	0.0	0.0	0.0	0.0
29	3.09	0.0	0.0	0.0	0.0
30	3.15	0.0	0.0	0.143	0.170
31	6.45	0.0	0.0	0.0	0.0
32	29.3	0.0	0.0	0.0	0.0
33	0.1	0.0	0.0	0.0	0.0
34	0.1	0.4	0.8	0.0	0.0
35	0.1	0.4	0.8	0.0	0.0
36	4.0	0.4	0.8	9.0	9.0
37	4.0	0.0	0.0	0.0	0.0
38	10.	0.4	0.8	0.0	0.0
39	10.	0.4	0.8	0.0	0.0
40	10.	0.4	0.8	0.0	0.0

5. Calculated Results and Discussion

The sequence of events for the present analysis is compared with that in the experiment in Table 5.1. It is remarkable that the time of ACC injection initiation and the core reflood time were well simulated by the THYDE-P. The detailed discussion on the events in the table will be made in the following subsections.

5.1 Temporal Behavior of Pressure

The calculated pressure just above the active core (node 31) is shown in Fig. 5.1 along with the experimental data. It goes without saying that the calculated depressurization process is highly dependent on the break flow simulation model. Therefore, it colud be said that the present break flow model in THYDE-P with the discharge coefficient 0.8 gave a good agreement with the experimental depressurization process. The calculated break flows will be directly compared with the experimental data in Subsec. 5.5.

End of blowdown, which is often defined as the time when the system pressure has almost decreased to the containment pressure, might be defined as about 35 sec. after rupture in both the experiment and the calculation.

5.2 Cladding Surface Temperature and Thermal-Hydraulic Behavier in Core

5.2.1 Overall Trend

The cladding surface temperatures at nodes 26, 27 and 28 are shown in Figs. 5.2.1, 5.2.2 and 5.2.3, respectively, along with the experimental data, where the heights of the measurment points from the bottom of the core are nearly equal to those in the analysis, and their horizontal locations in the core are chosen from the seemingly average bundle. The heat transfer coefficient calculated at node 27 is shown in Fig. 5.3, where the heat transfer modes (see Tables 3.1.1 and 3.1.2) are shown. The calculated mass flux and coolant qualities at core node 27 are shown in Figs. 5.4 and 5.5, respectively.

The averall trends of the calculated cladding surface temperatures are in good agreement with the experimental data in the sense that there are

peakes during the blowdown and the final quenching was calculated to occor at about 50 sec. after rupture. The reason why the peakes during the blowdown were calculated will be explained in the following subsection .

In the experiment, DNB was observed at about 20 sec. and also in the analysis DNB occured at about 18 sec. under the pool flow condition, where the CHF value was predicted by the modified Zuber correlation[16][17]. At about 30 sec. in the calculation, the core nodes became superheated and the heat transfer coefficients suddenly decreased and the cladding surface temperature increased. After about 40sec. the effects of ECC water became apparent and the core nodes returned to be saturated. As shown in Fig. 5.5, the coolant quality at node 27 became under x_c (=0.1) and then the heat transfer mode changed from mode 4.4 (pool film boiling) to mode 4.5 (pool transition boiling). The sudden decrease in the calculated cladding surface temperature was brought about by the mode transition and then the final quenching, the mode transition to mode 3 (nucleate boiling), occured .

5.2.2 Detail of Blowdown

The calculated cladding surface temperatures, heat transfer coefficients at the core nodes at the very early stage of the blowdown are shown in Figs. 5.6 and 5.7, respectively. The mass fluxes at the inlet and the outlet of node 27 are shown in Fig. 5.8, where the pool flow condition is denoted.

As shown in Fig. 5.6, two prominent peakes of the cladding surface temperatures appeared at node 27 and 28. The reason may be clarified by Figs. 5.7 and 5.8. DNB was calculated to occur twice at about 0.6 and 0.8 sec. in conjunction with flow stagnation and quenching was also calculated to occur twice at about 1.2 and 3 sec., under the forced convection condition. It could be said, therfore, the rewetting phenomena observed in the blowdown might be brought about by the large forward core flow due to the effects of the primary coolant pumps, which were running until 200 sec. after rupture.

5.2.3 Coolant Temperature at Upper Plenum

The coolant temperature calculated just above the active core, at node 31, is shown in Fig. 5.9 along with the experimental data. As observed

in the experiment, primary coolant in the upper plenum departed from the saturated state at about 30 sec. and stayed at the superheated state unitl about 40 sec. Also in the analysis, the superheated state was calculated to exist intermittently from 30 to 40 sec. The calculated results are well understood from the fact that coolant at the active core nodes became superheated at about 30 sec. and returned to be saturated at about 40 sec. due to the effects of ECC water as stated in Subsec. 5.2.2.

5.3 Intact Loop Cold Leg and Accumulator Injection

In Fig. 5.10, the calculated ACC pressure is compared with the experimental data, where the calculated loop pressure near the ECC water injection point, node 20, is shown. The calculated injection mass flow rate from the accumulator is shown in Fig. 5.11 along with the experimental data. Overall trend of the accumulator was well simulated by the present calculation. The calculated coolant enthalpies at the accumulator and node 40, which simulated ACC piping, are shown in Fig. 5.12. It took about 10 sec. for the coolant enthalpy at the ACC side of node 40 to decrease to the value of the accumulator enthalpy, about 30 kcal/kg.

The calculated coolant density at node 21 which is located downstream of the ECC injection point is shown in Fig. 5.13 along with the experimental data. In the calculation, the node became filled with subcooled water at about 25 sec. due to ACC injection. On the other hand in the experiment, many sharp peakes, which imply the existence of slugs or drops, were observed. It is of no use to say that thermal non-equilibrium effects due to low enthalpy ACC water were considerably large in this time period. Generally, analyses of this time period by thermal equilibrium models fail because of overestimated condensation rates. In the present analysis, the difficulty was avoided by applying the time delay model for density change (see subsec. 3.4), where the value of the delay parameter at node 20 was about 1 sec. The calculated mass fluxes at node 20 are shown in Fig. 14. It is shown in the figure that coolant in node 20 once became subcooled and again returned to be saturated.

The calculated coolant temperatures at the intact loop hot and cold legs, node 11 and node 21, are shown in Fig. 5.15 along with the experimental data.

The existence of subcooled water in the intact loop cold leg is clearly shown in both the experimental and calculated curves after the ACC injection initiated.

5.4 ECC Water Penetration through Downcomer

The calculated mass flow rates and coolant enthalpies at the inlet and the outlet of the downcomer node, node 22, are ahown in Figs. 5,16 and 5.17, respectively. The curves show that ECC water penetration through the downcomer node started at about 30 sec. but it was premature. The constantly forward flow at the inlet of the downcomer was established at about 36 sec. and then coolant became subcooled at about 40 sec. The reason why the inlet mass flow rate was much larger than the outlet mass flow rate even after 40 sec. is that due to the non-equilibrium model applied, the void fraction was gradually decreasing to zero during this period.

The calculated coolant temperature at the downcomer was shown in Fig. 5.18 along with the experimental data. In the experiment, subcooled water was observed first several seconds after the ACC injection initiated, i.e. the late portion of the blowdown phase. On the other hand in the analysis, only overall trend was analysed since the downcomer was simulated by a single node.

5.5 Broken Legs and Break Flows

The mass flow rates at the broken legs are shown in Figs. 5.19 and 5.20 along with the experimental data. At the early stage of the blowdown, the break flow at the hot leg was overestimated while it was underestimated at the cold leg. The coolant densities at the broken hot and cold legs are shown in Figs. 5.21 and 5.22, respectively, along with the experimental data. The coolant density at the cold leg was overestimated throughtout the calculation (see Fig. 5.22). The overestimation of the break flow at the cold leg during the period from 10 to 35 sec. (see Fig. 5.20) might be brought about by this overestimation of the coolant density, namely the underestimation of the coolant enthalpy at the broken cold leg. The major reason for the underestimation of the coolant enthalpy is thought to exist in the nodalization for the downcomer region. Two-dimensional effects in the downcomer, which couid be evaluated to some extent

for example, by nodalizing the downcomer into more than two nodes azimuthaly, might have to be taken into consideration. Another reason for the underestination of the coolant enthalpy at the broken loop cold leg was that heat transfer between coolant and structure was neglected in the present analysis. In the refill-reflooding phase, the mass flow rate at the leg considerably decreased and therefore heat input to coolant from the duct wall might have played an important role.

5.6 Steam Generator

The calculated heat inputs from the SG secondary system to primary coolant at nodes 14 and 15, which simulated U-tubes, are shown in Fig. 5.23. The SG secondary system was calculated to change from heat sink to heat source to the primary coolant at about 15 sec. after rupture. The calculated SG secondary pressure is shown in Fig. 5.24 along with the calculated primary side pressure. The figure 5.25 shows the calculated coolant temperatures at both the inlet plenum and the outlet plenum of the steam generator. The outlet plenum (node 16) was filled with superheated steam at 25 sec. in the present analysis.

5.7 Pressurizer and Intact Loop Hot Leg

The calculated pressures at the intact loop hot leg (node 2) and the pressurizer are shown in Fig. 5.26, along with the experimental data. The loop pressure was in good agreement with the experimental data but the pressurizer pressure was not. One of the reasons for the discrepancey was that the initial water temperature of the pressurizer was considerably lower than the experimental value (see Table 4.1). The code modification with respect to the problem has been done in the most update version of THYDE-P.

5.8 Primary Coolant Pumps

The calculated pump normalized speed, flow and head are shown in Figs. 5.28, 5.29 and 5.30, respectively. In the experiment, the pumps were running until 200 sec., and therefore pump speeds were assumed to be constant in the present calculation. Although the pumps might have played an important role in conjunction with the rewetting phenomena during the blowdown phase, few experimental data for the pumps were available.

Table 5.1 Sequence of Events for LOFT L2-3

Event	Time afetr Blowdown Initiation (sec)	
	Experiment	Present Analysis
LOCE L2-3 initiated	0.0	0.0
Reactor scram signal recieved at control room	0.103	0.103
Control rod completely incerted	1.683	not clear
HPIS injection initiated	14.	14.[a]
Pressurizer emptied	14.	not clear
Accumulator injection initiated	17.	16.3
LPIS injection initiated	29.	29.[a]
Lower plenum filled with liquid	35.	40.
Accumulator liquid line flow ended	49.	not clear
Core volume reflood	55.	60.

(a) These values were set by inputs.

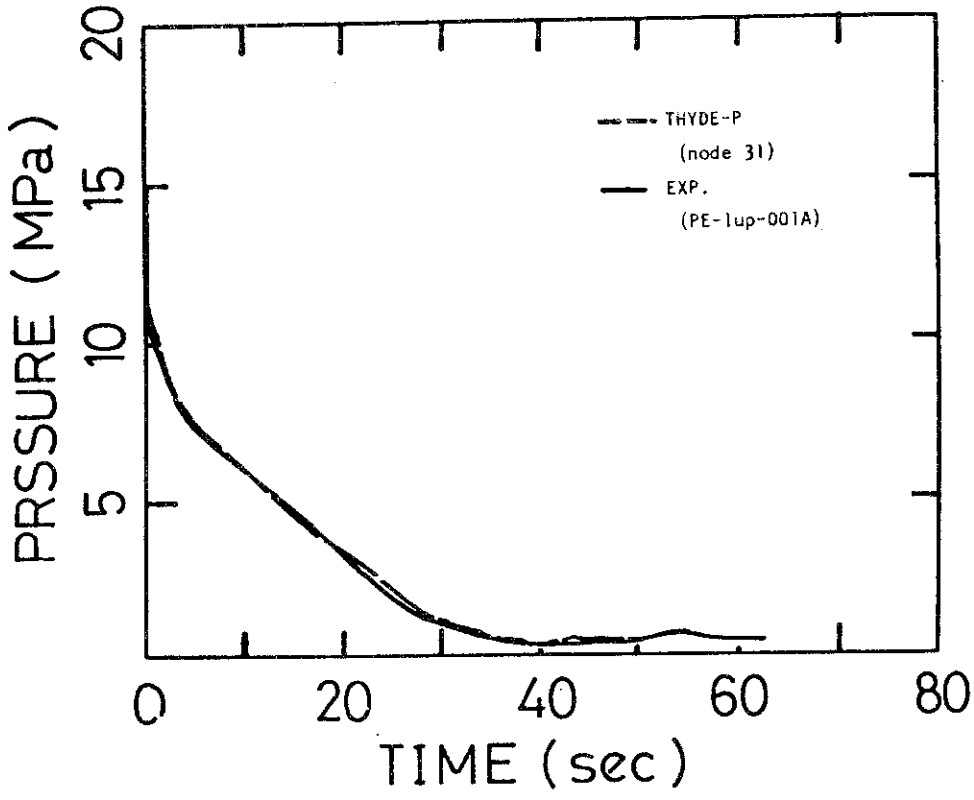

Fig.5.1 Temporal behavior of Pressure

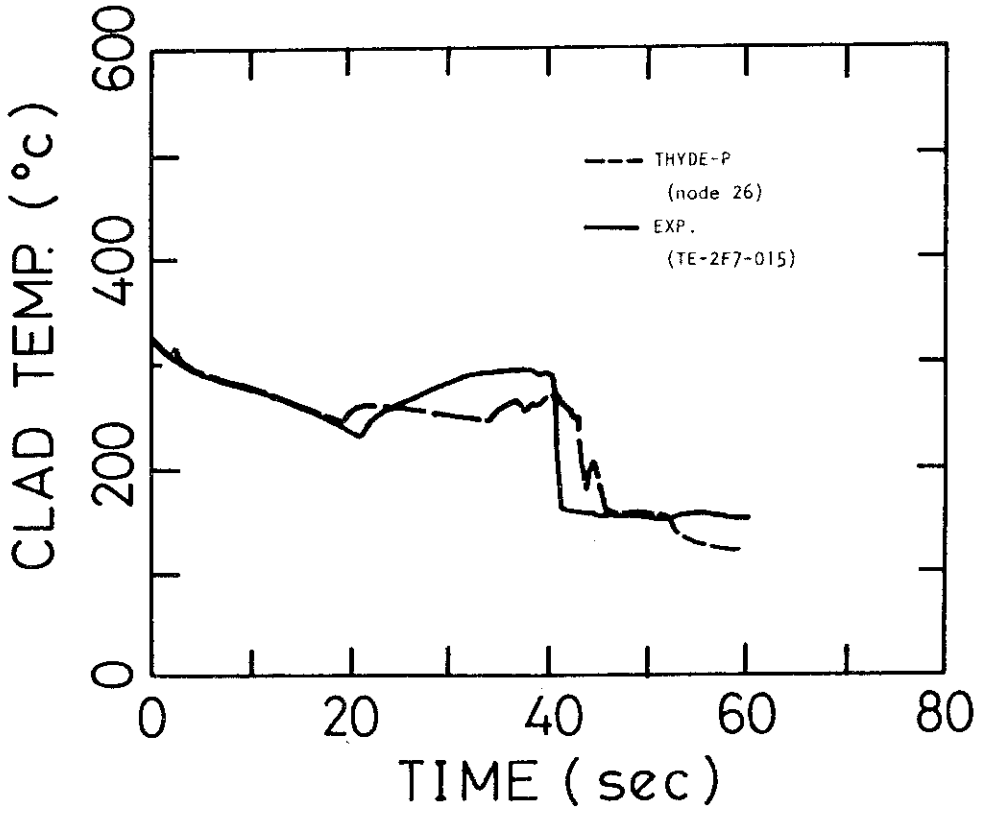

Fig.5.2.1 Cladding Surface Temperature (Node 26)

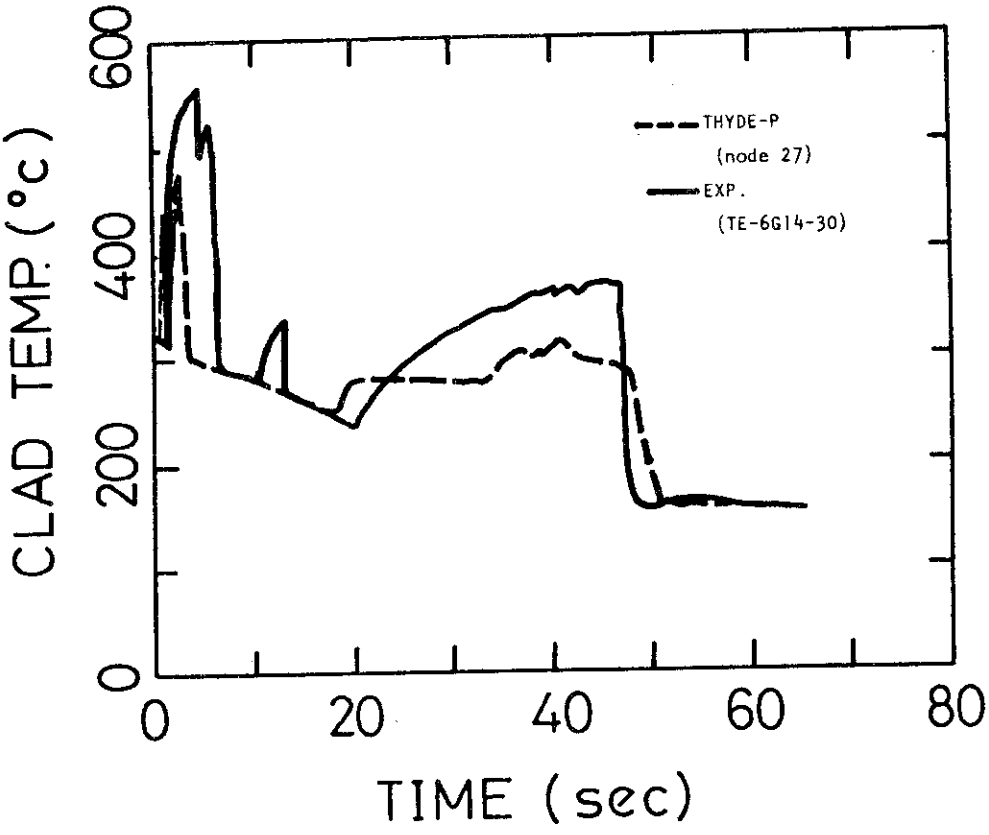

Fig.5.2.2 Cladding Surface Temperature (Node 27)

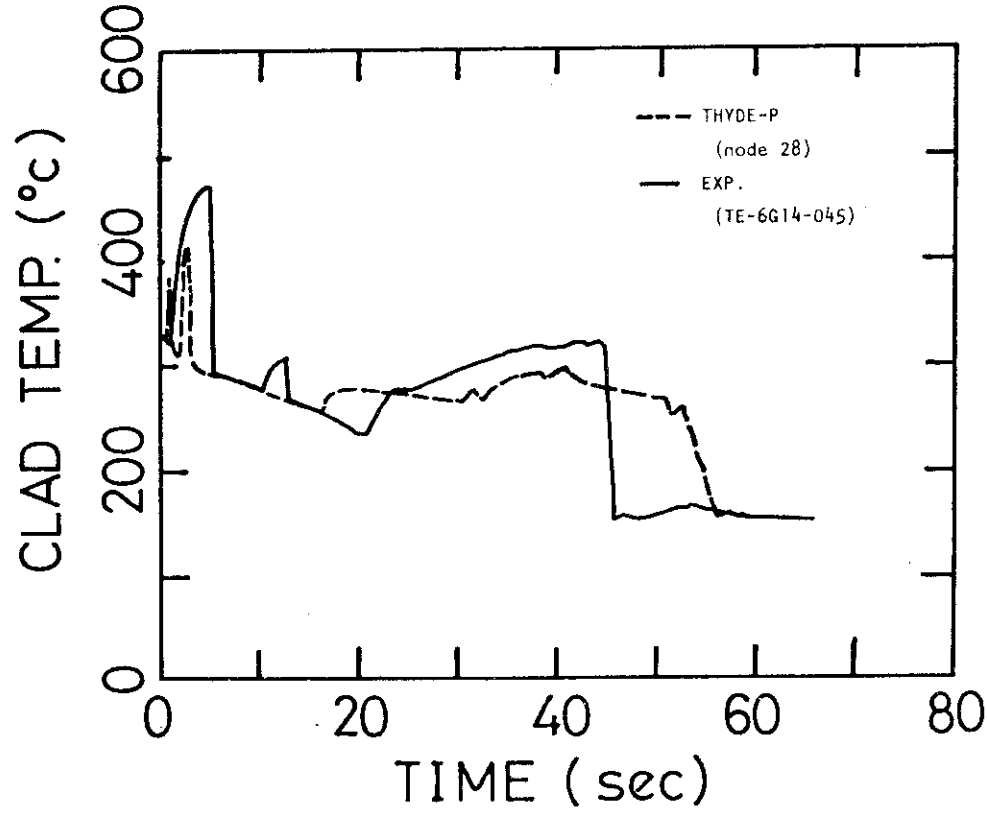

Fig.5.2.3 Cladding Surface Temperature (Node 28)

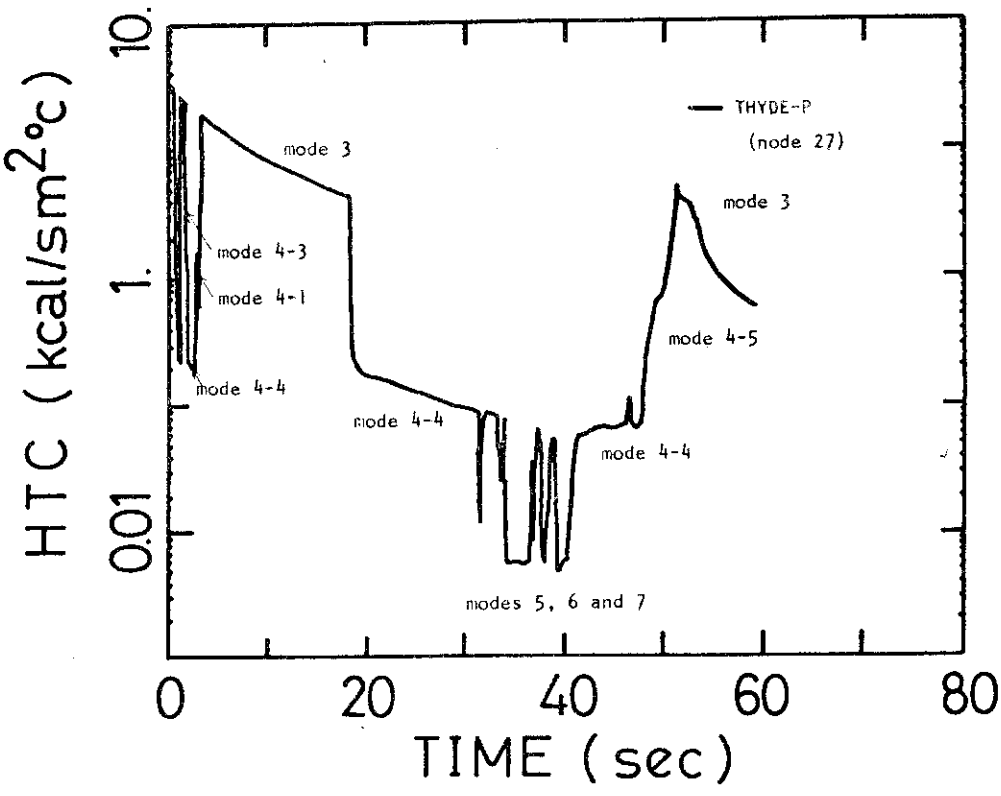

Fig.5.3 Calculated Heat Transfer Coefficient at Core Node 27

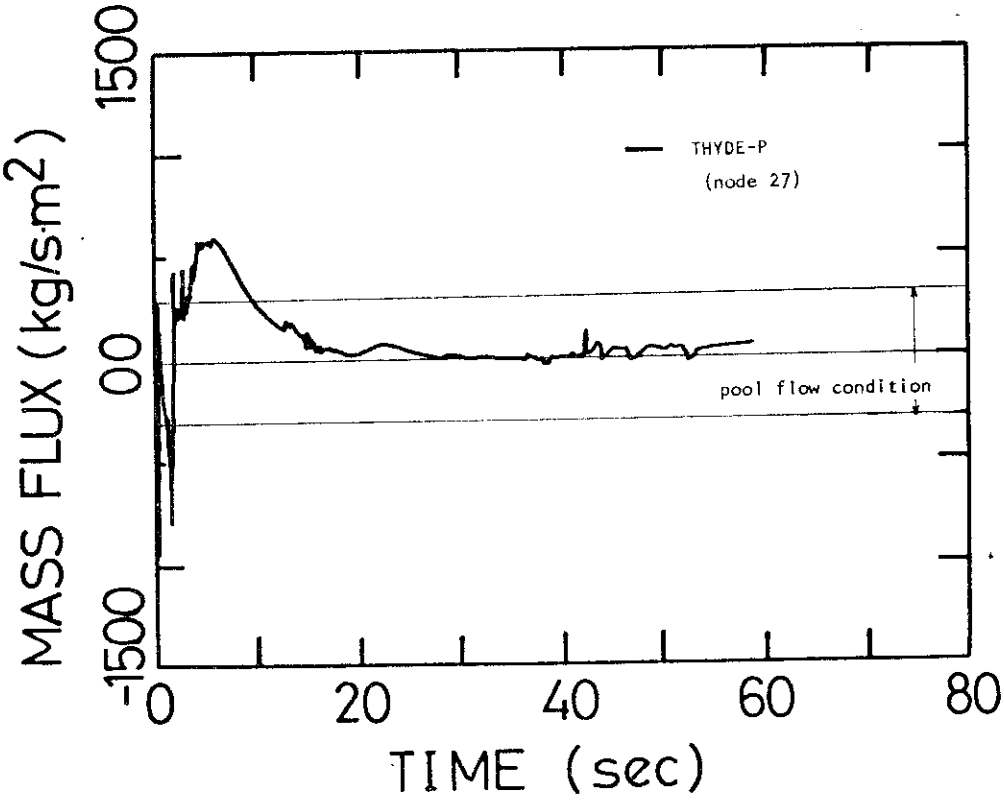

Fig.5.4 Calculated Mass Flux at Core Node 27

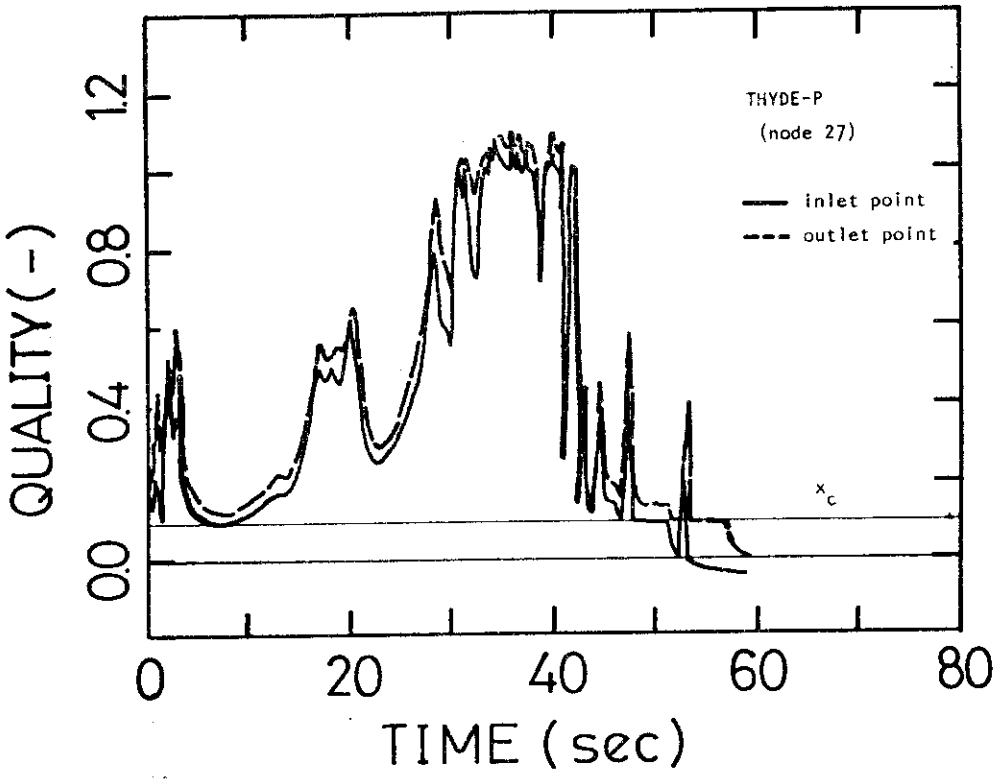

Fig.5.5 Calculated Coolant Qualities at Core Node 27

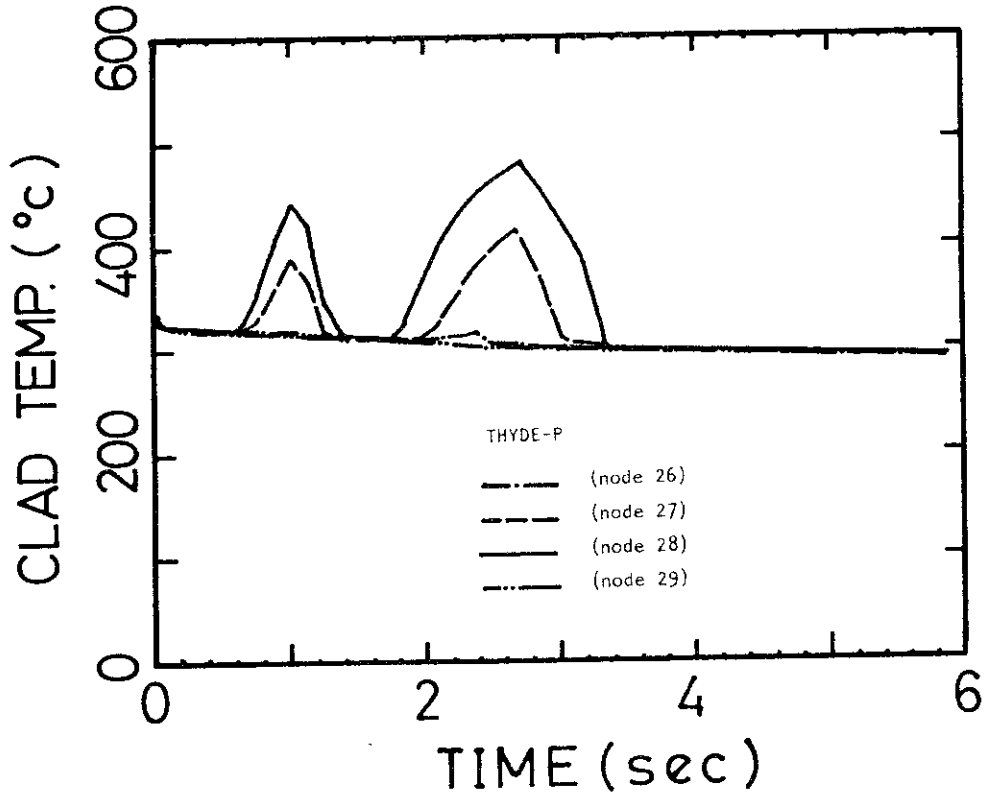

Fig.5.6 Calculated Cladding Surface Temperatures at Early Stage of Blowdown

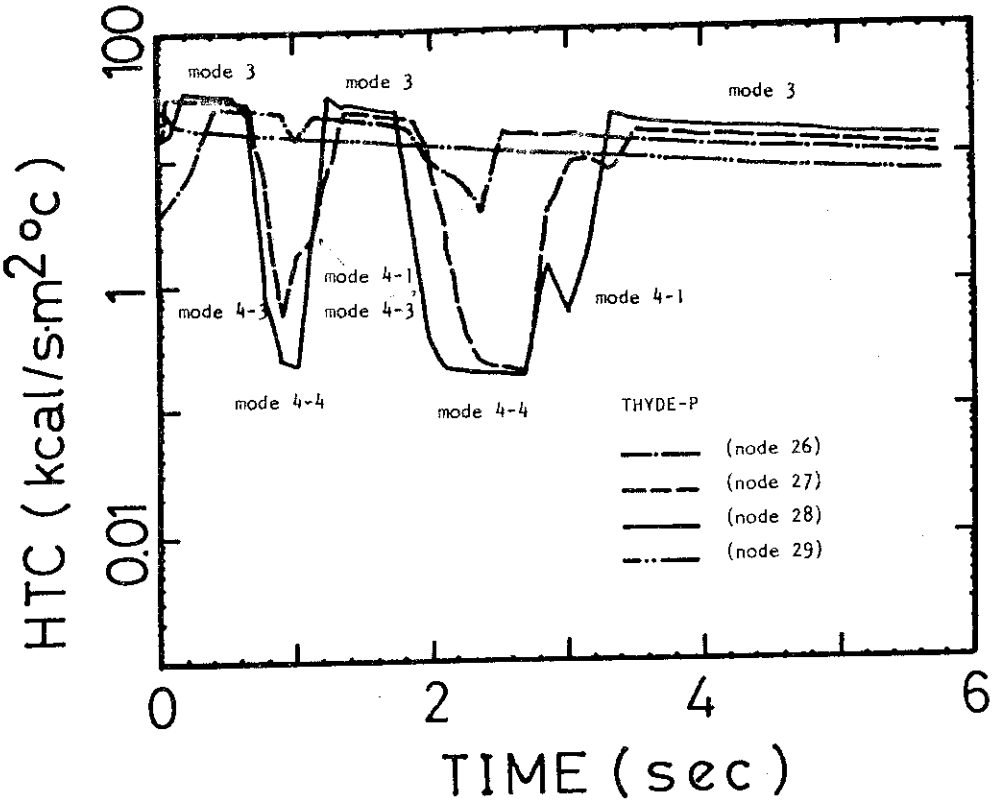

Fig.5.7 Calculated Heat Transfer Coefficients at Early Stage of Blowdown

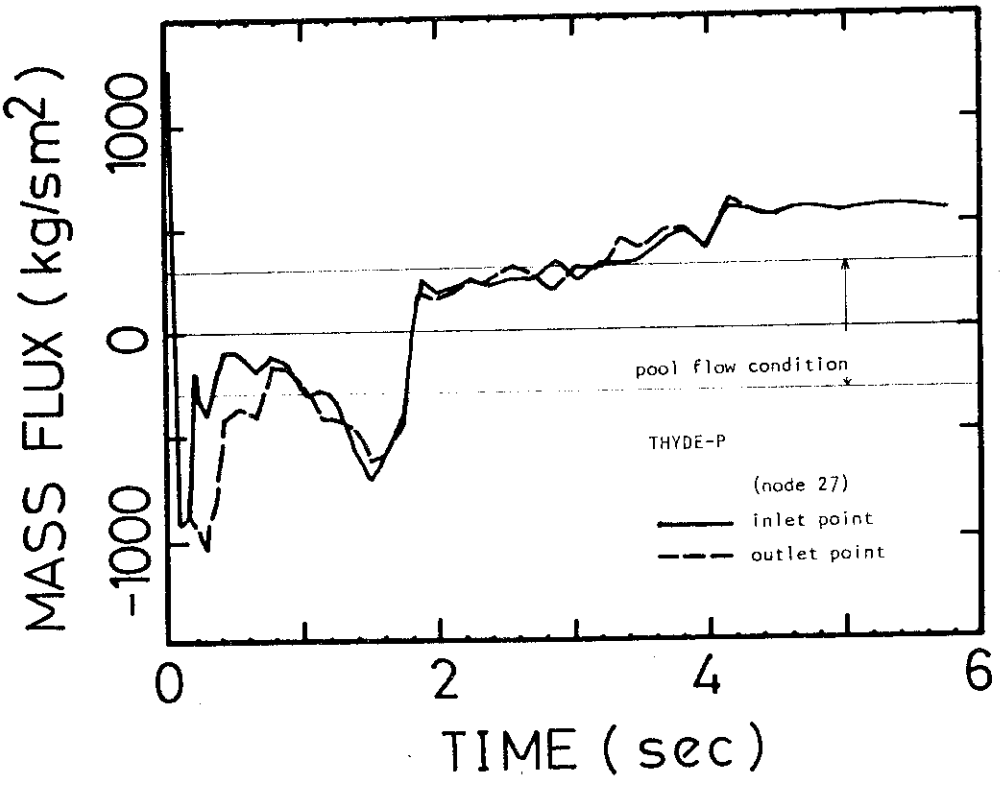

Fig.5.8 Calculated Mass Fluxes at Core Node 27 at Early Stage of Blowdown

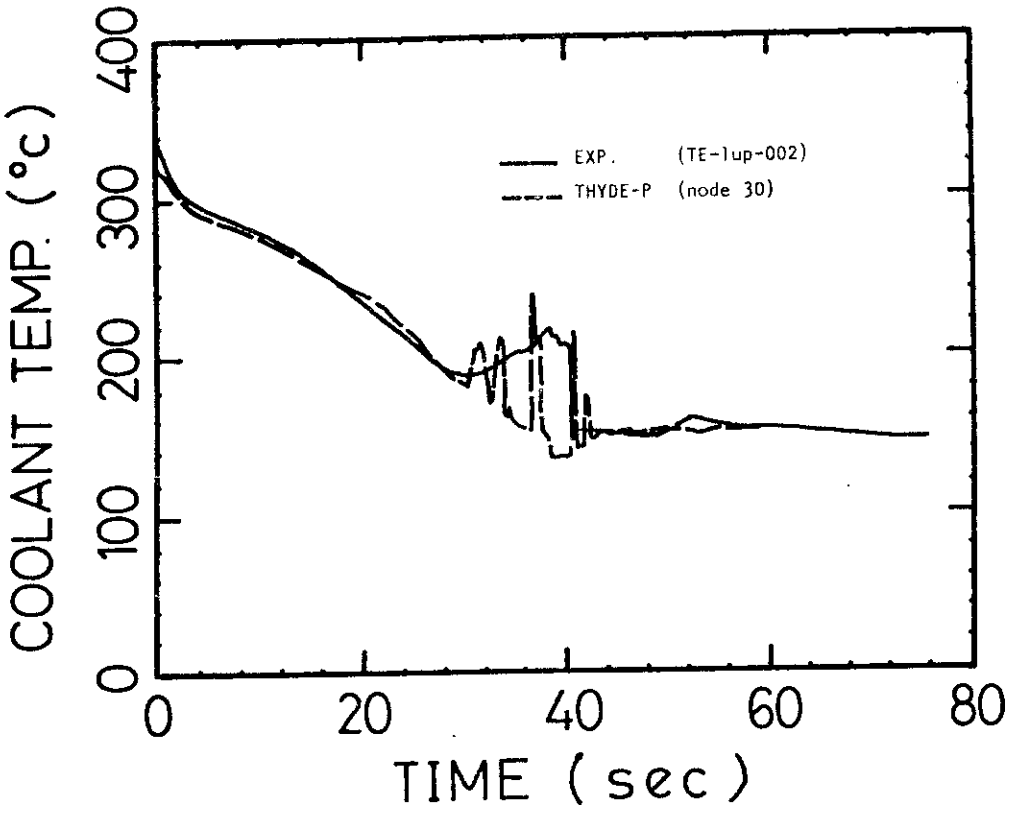

Fig.5.9 Coolant Temperature just above Active Core

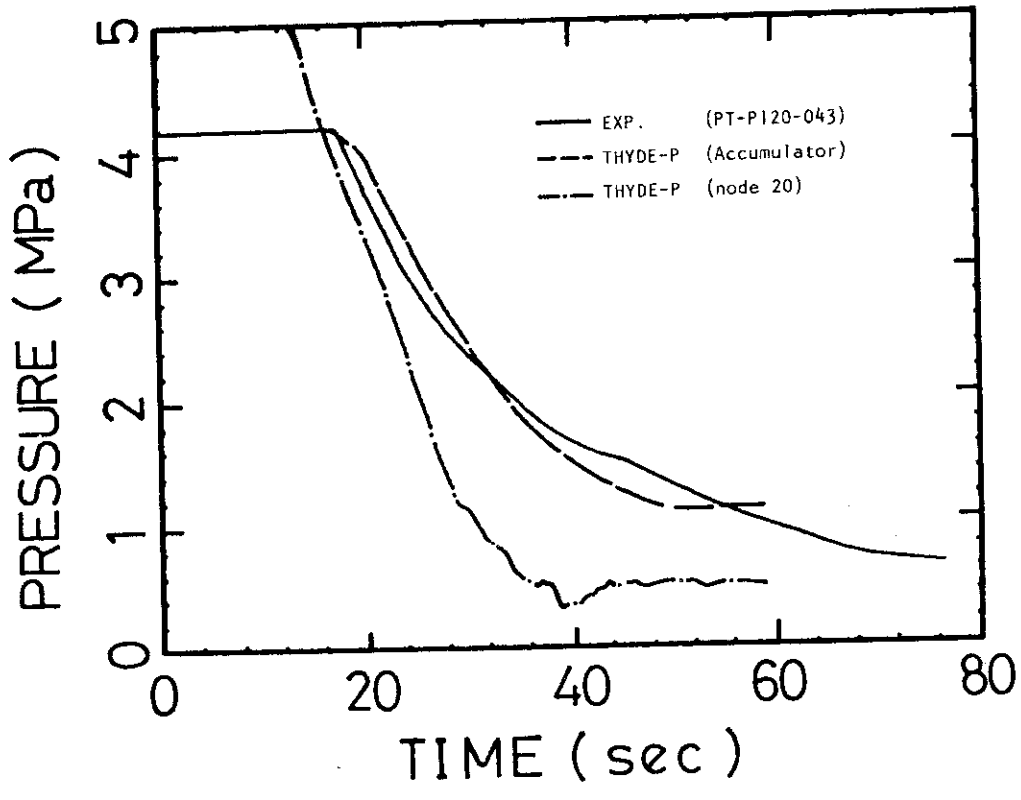

Fig.5.10 Accumulator Pressure

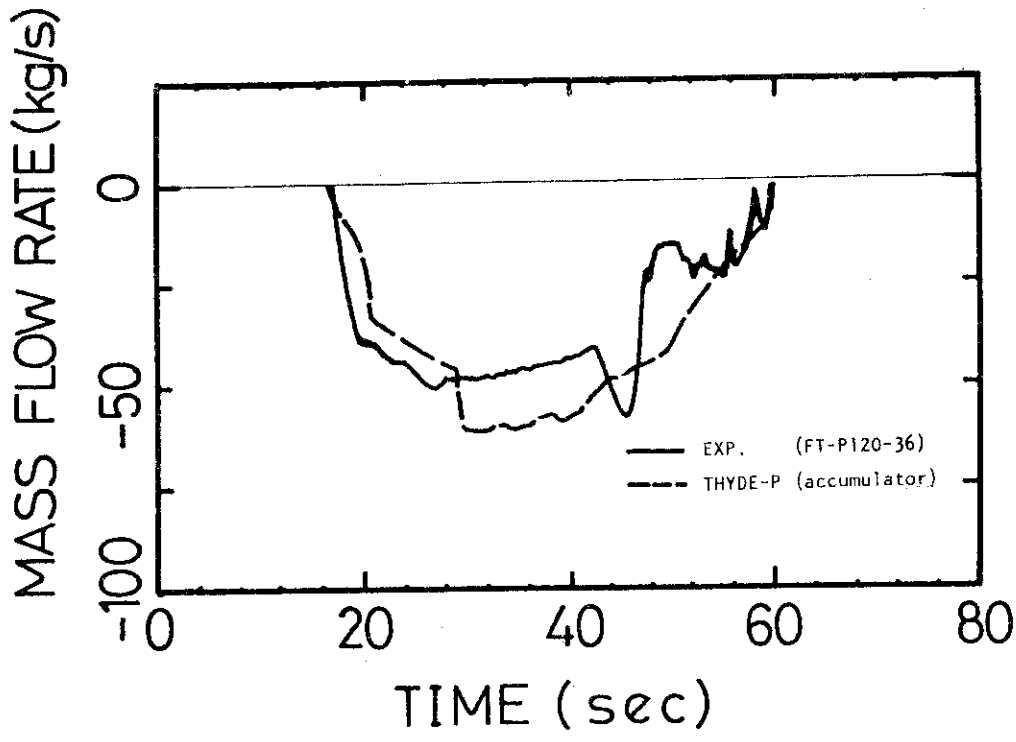

Fig.5.11 Injection Mass Flow Rate from Accumulator

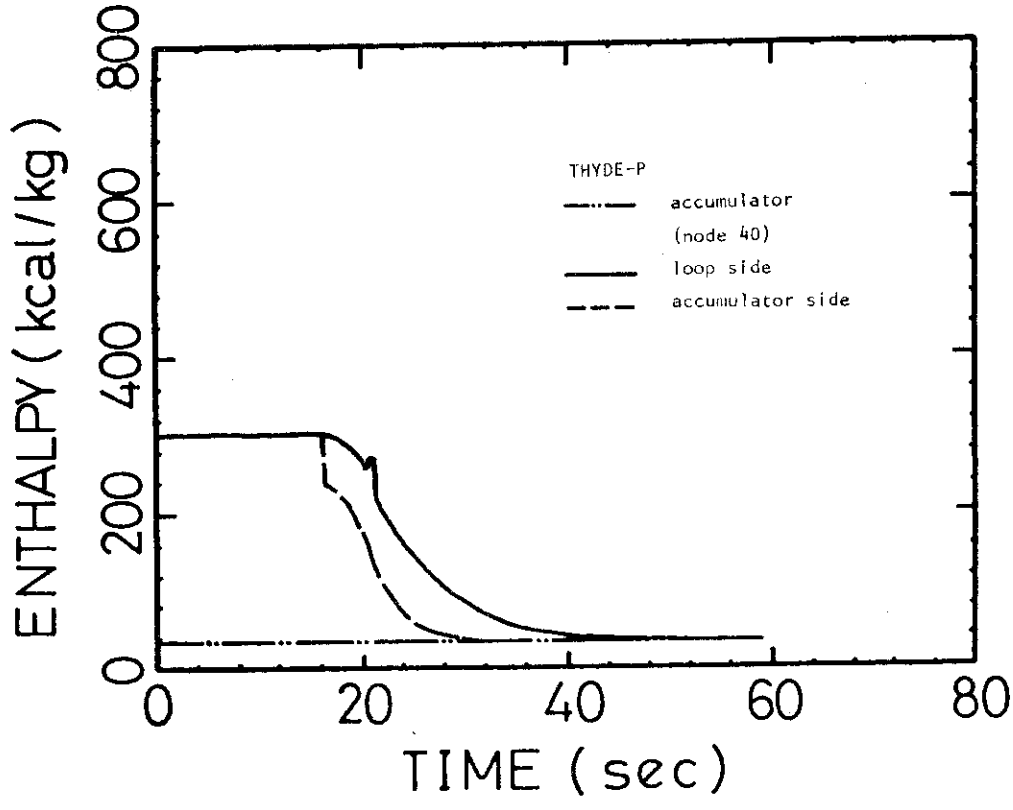

Fig.5.12 Coolant Enthalpies at Accumulator and Accumulator Piping

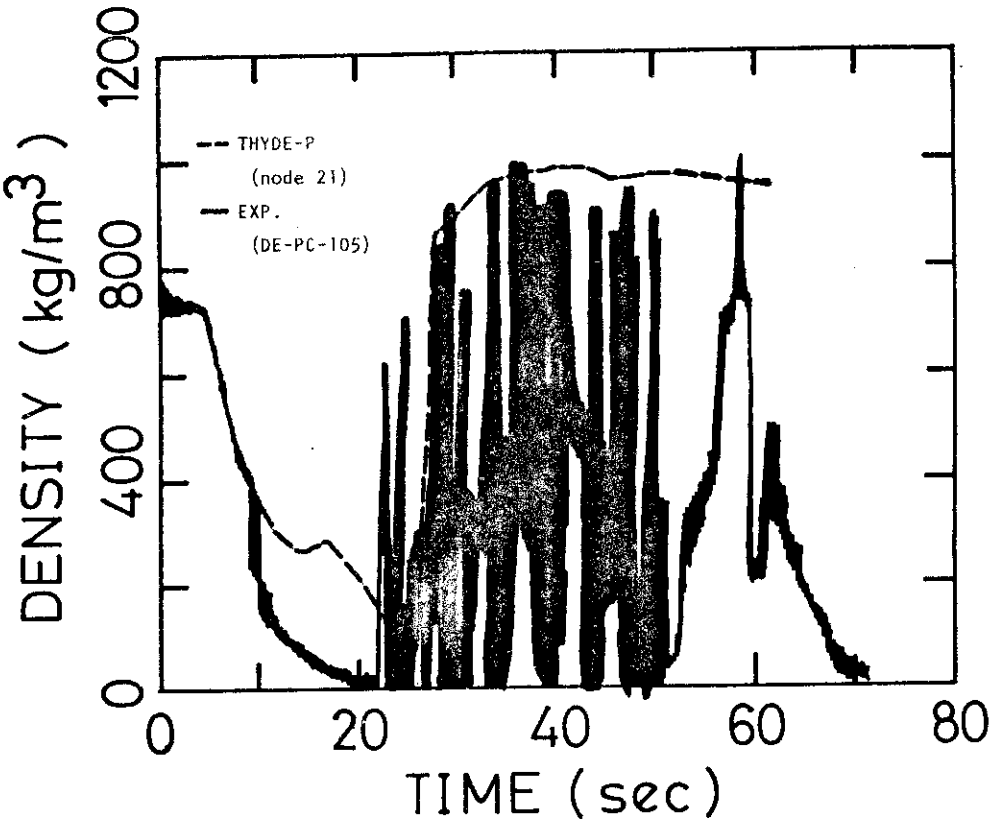

Fig.5.13 Coolant Density at Intact Loop Cold Leg

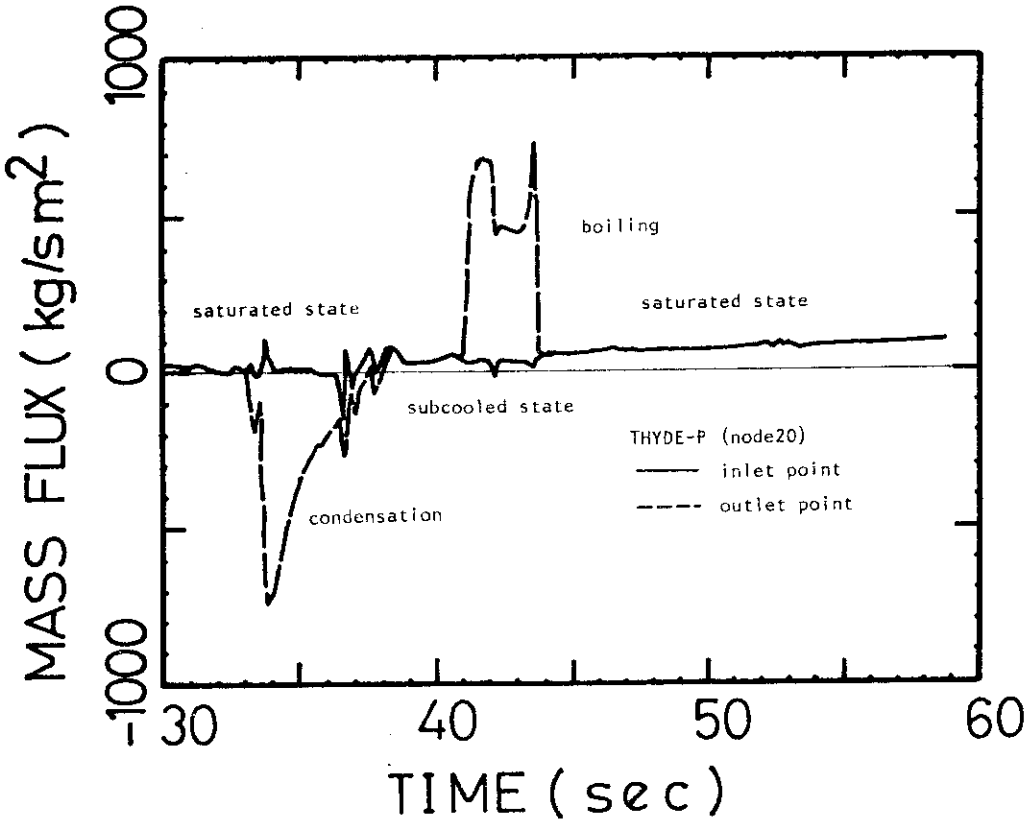

Fig.5.14 Calculated Mass Fluxes at Intact Loop Cold Leg (Node 20)

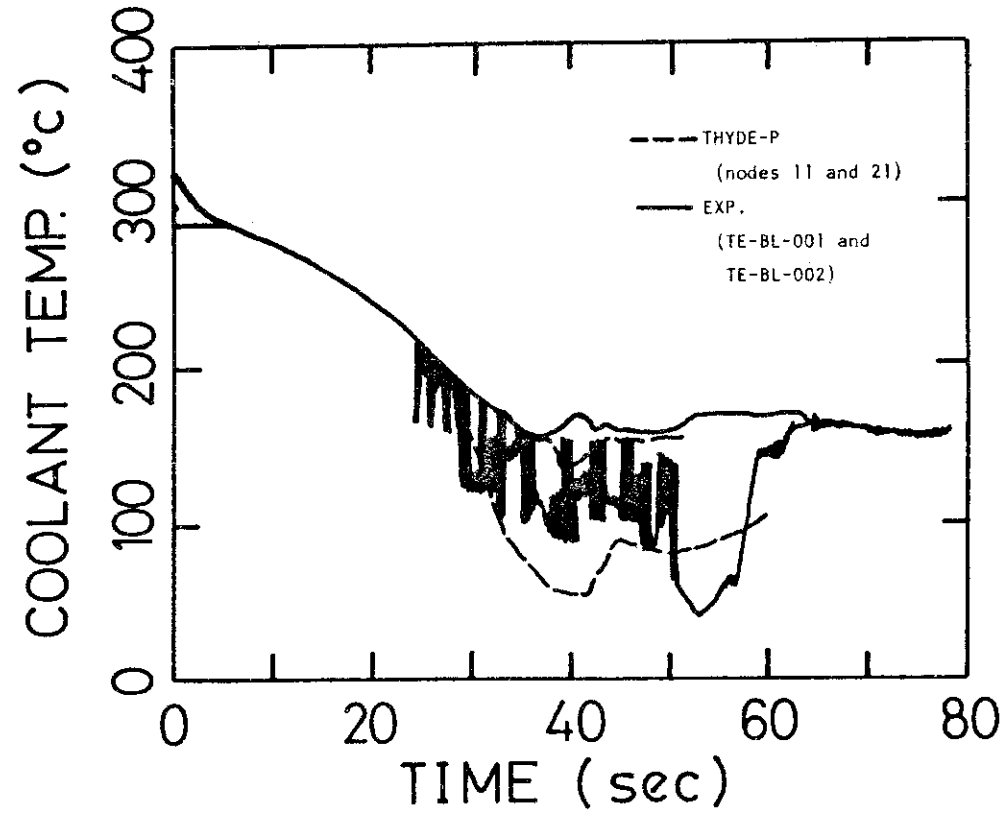

Fig.5.15 Coolant Temperatures at Intact Loop Hot and Cold Legs

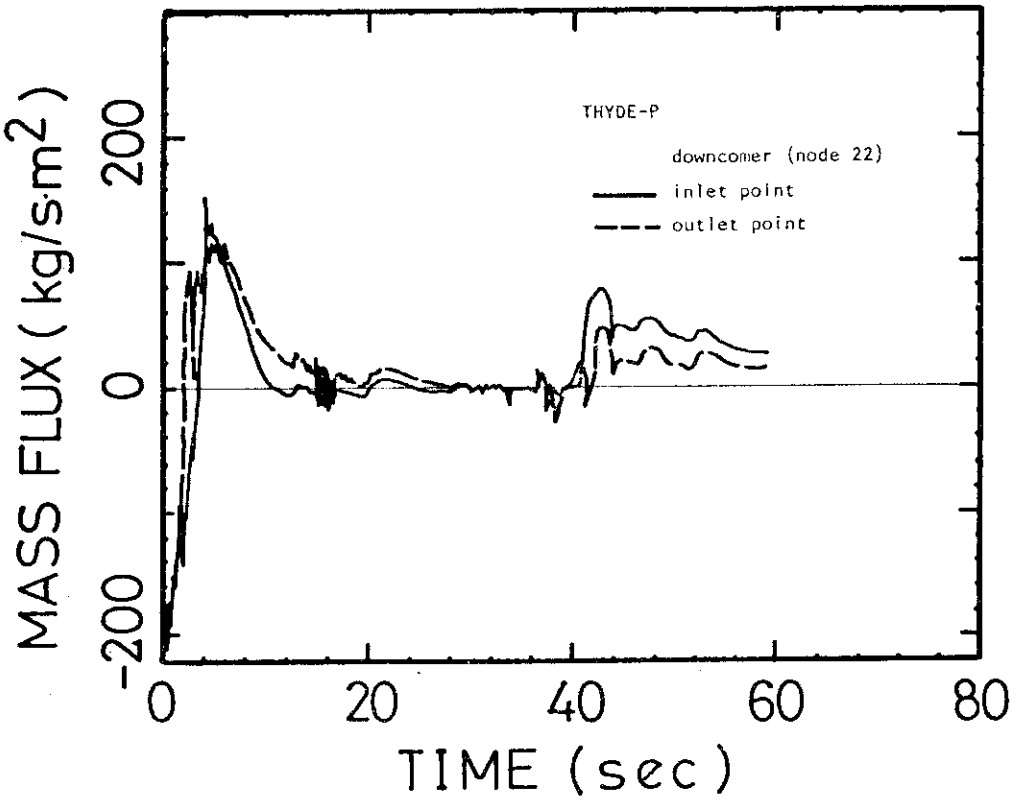

Fig.5.16 Mass Fluxes at Inlet and Outlet of Downcomer

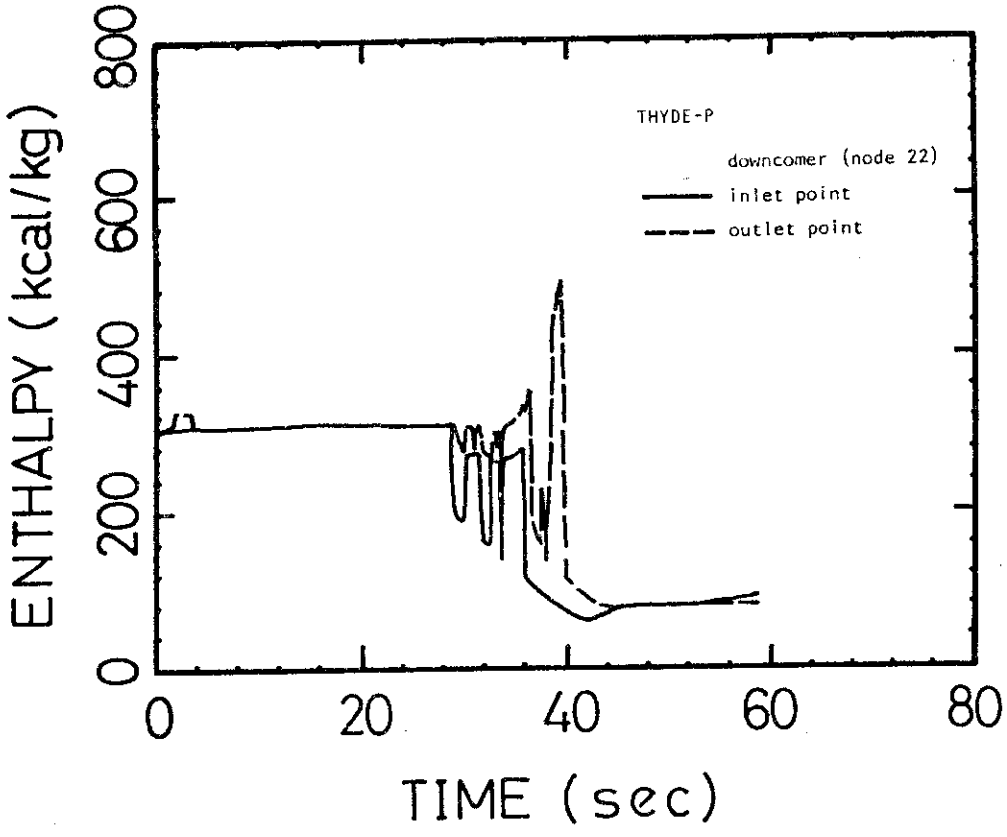

Fig.5.17 Coolant Enthalpies at Inlet and Outlet of Downcomer

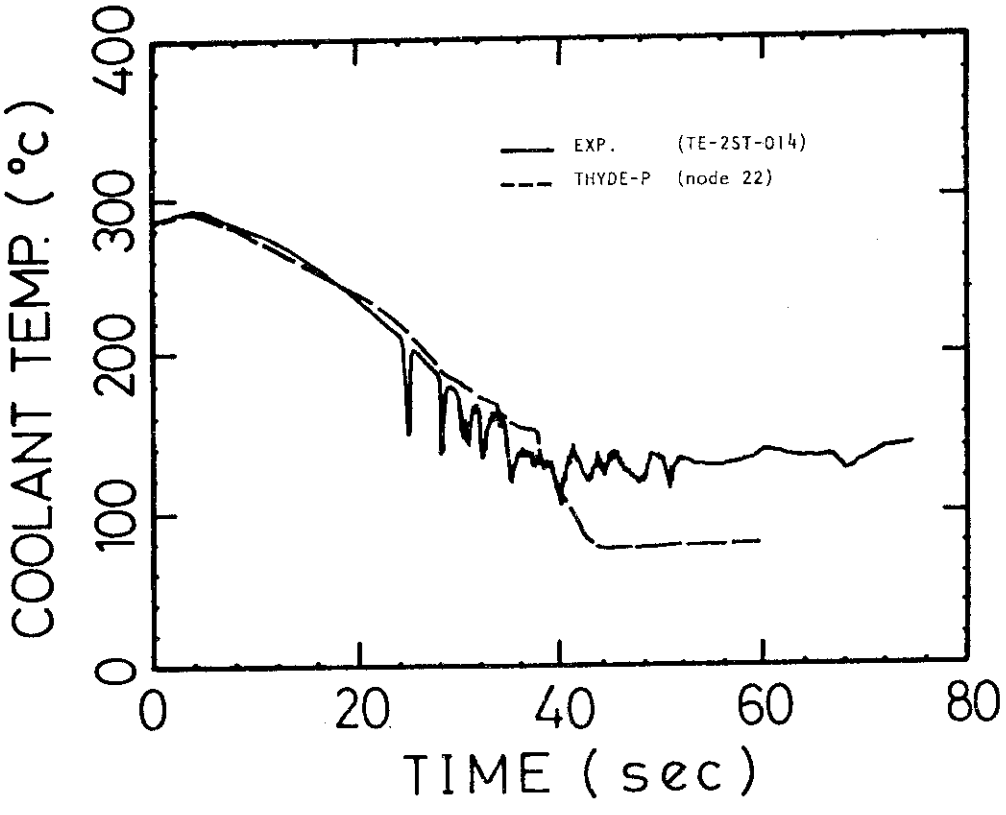

Fig.5.18 Coolant Temperature at Downcomer

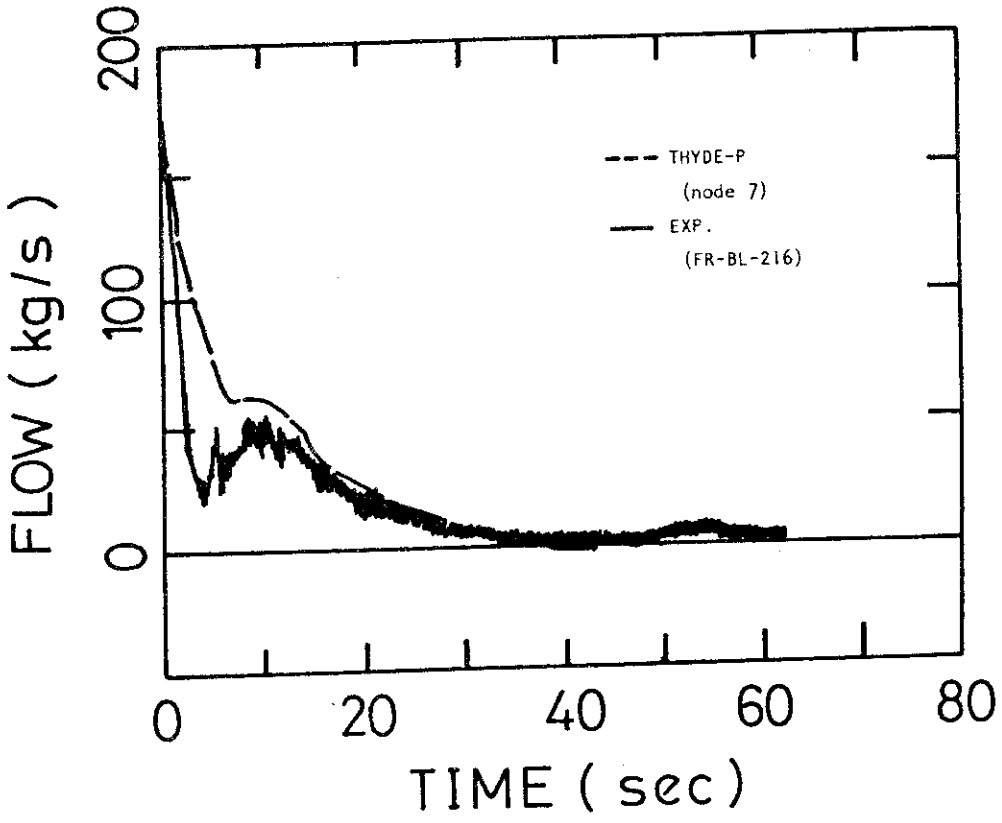

Fig.5.19 Break Flow at Hot Leg

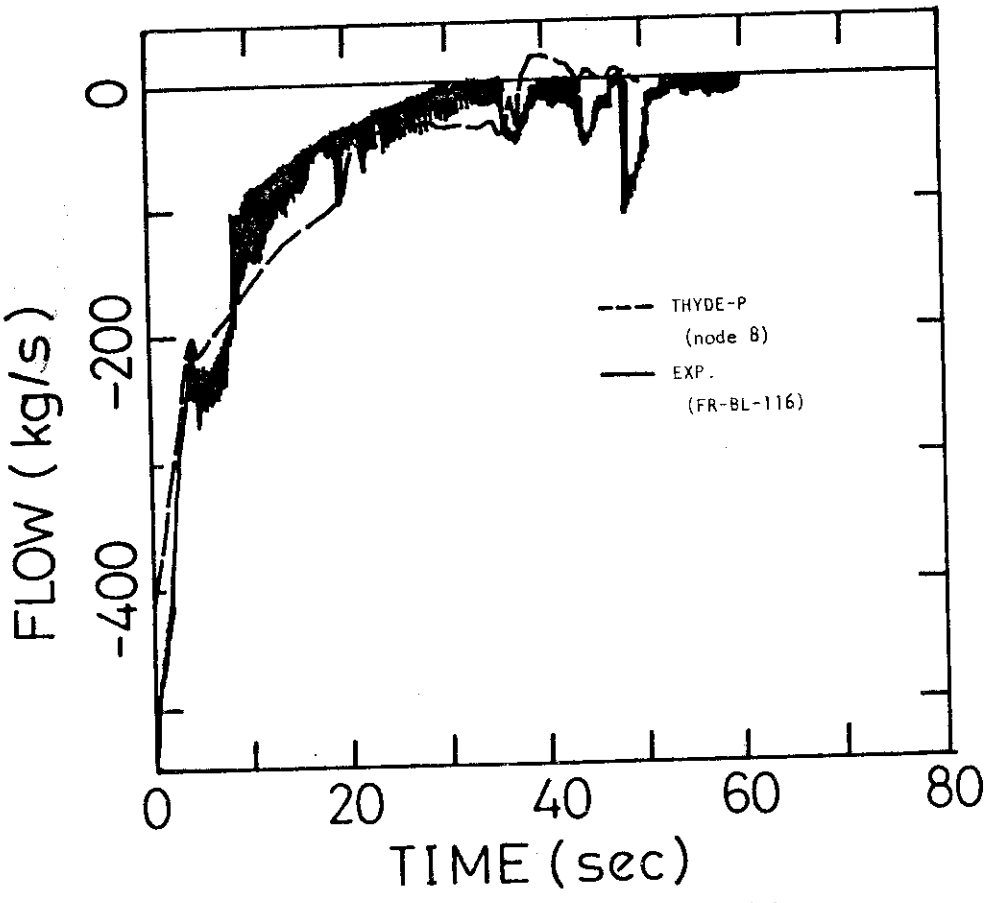

Fig.5.20 Break Flow at Cold Leg

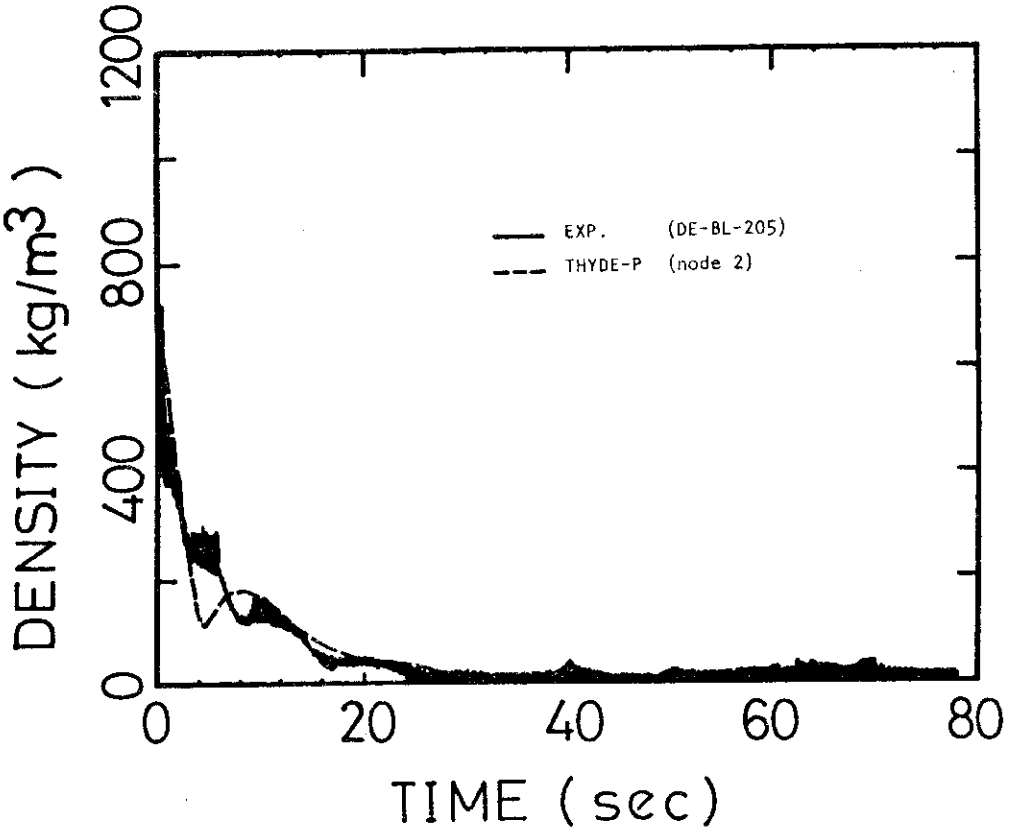

Fig.5.21 Coolant Density at Broken Loop Hot Leg

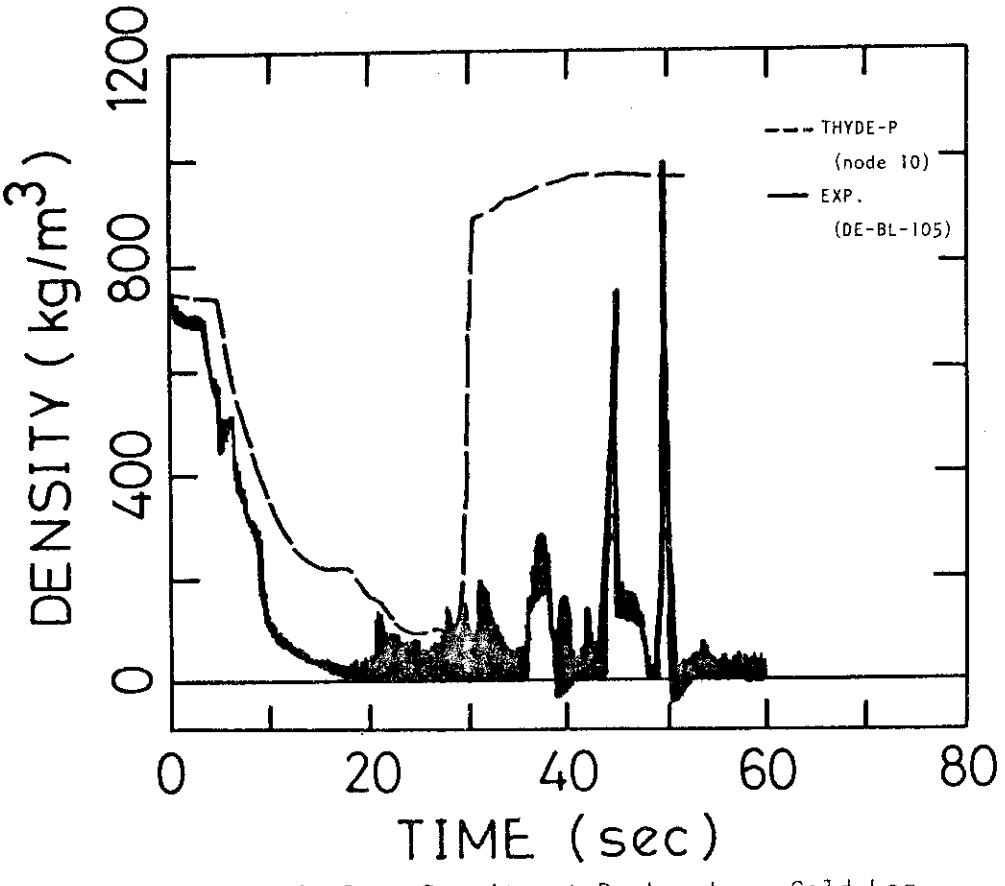

Fig.5.22 Coolant Density at Broken Loop Cold Leg

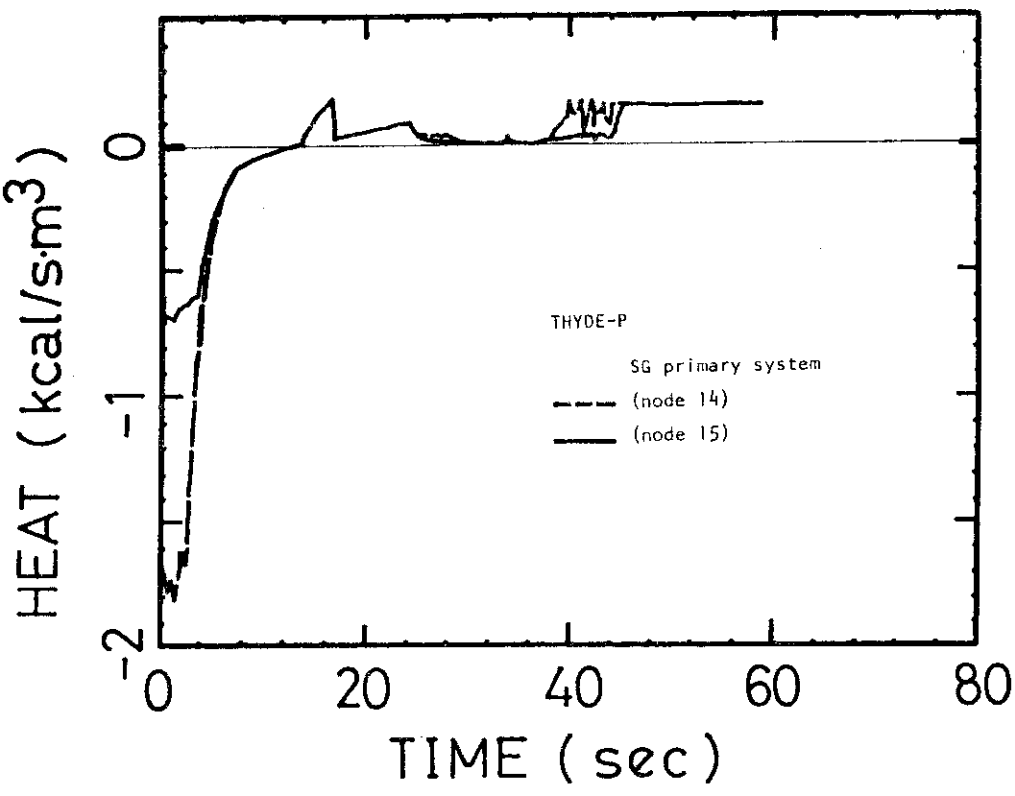

Fig.5.23 Heat Transfer from SG Secondary System to Primary System

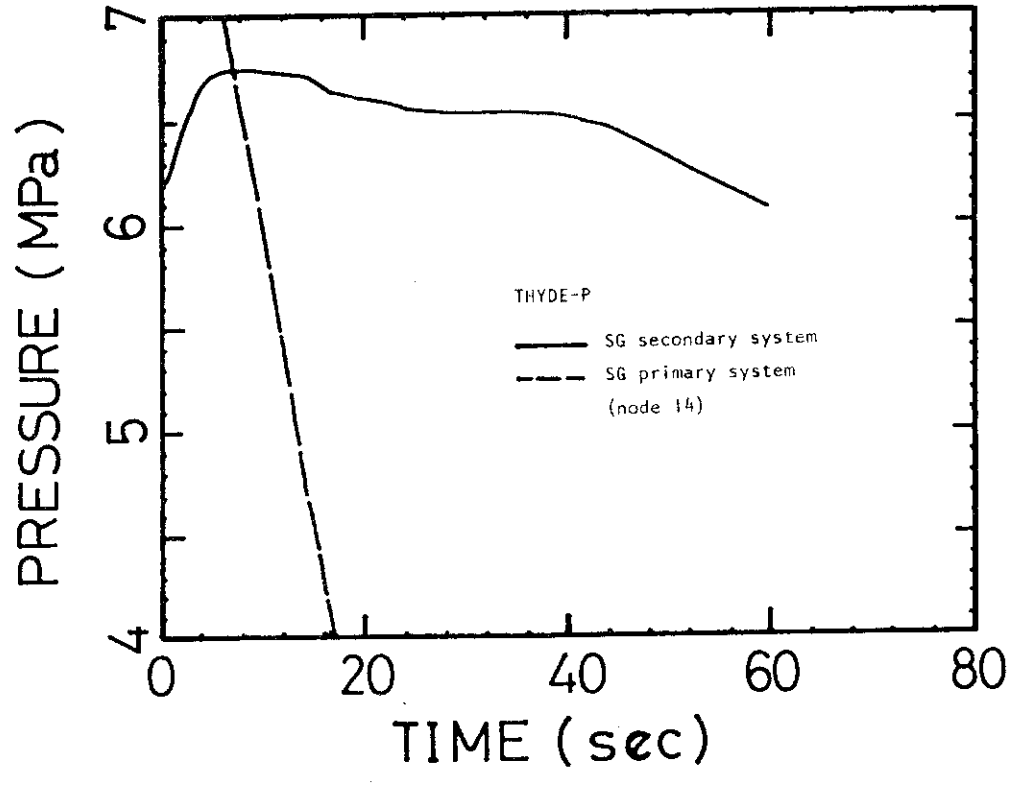

Fig.5.24 Calculated SG Secondary and Primary Pressures

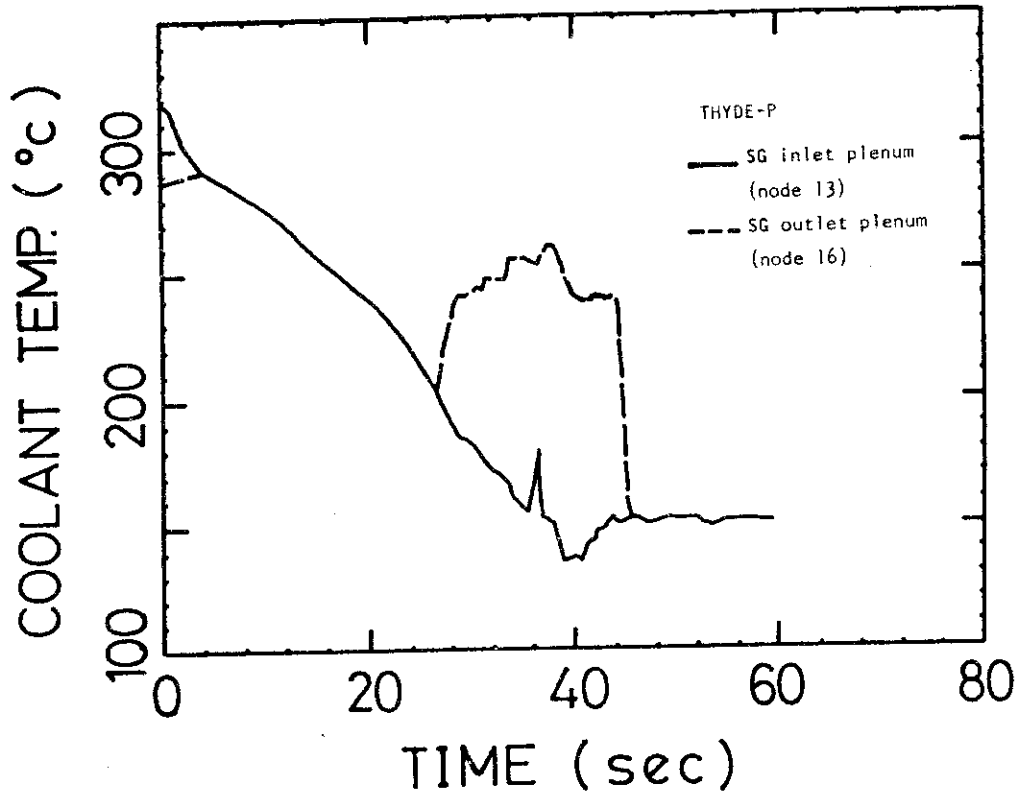

Fig.5.25 Calculated Coolant Temperatures at SG Inlet and Outlet Plenums

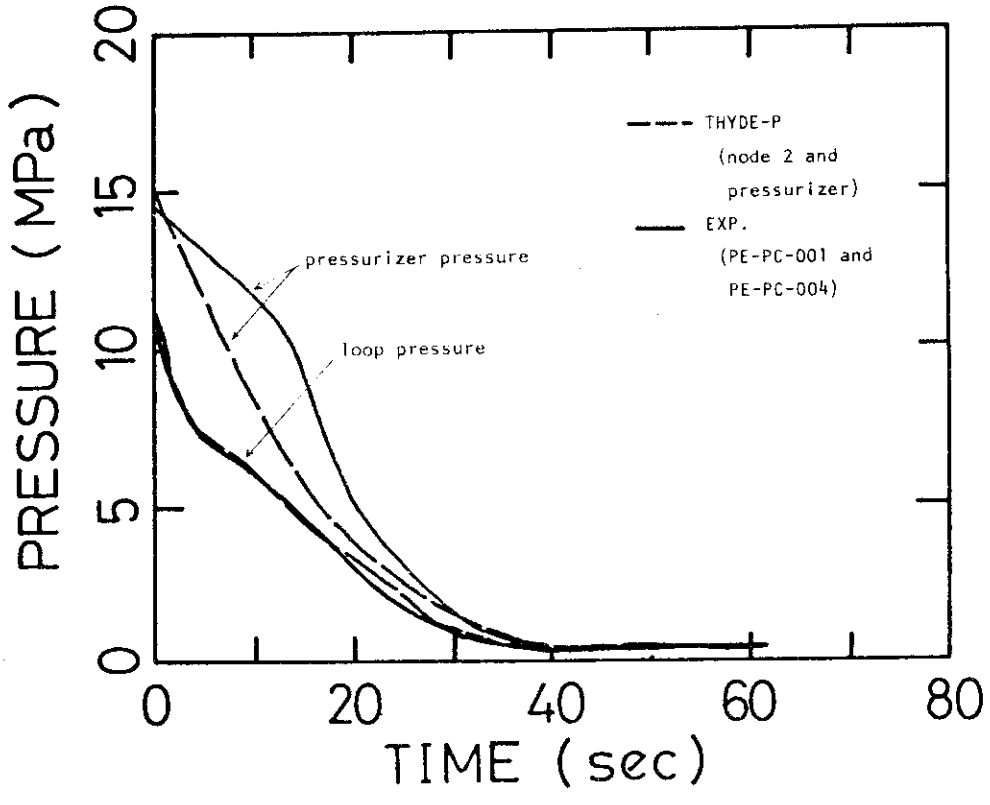

Fig.5.26 Pressurizer and Intact Loop Hot Leg Pressures

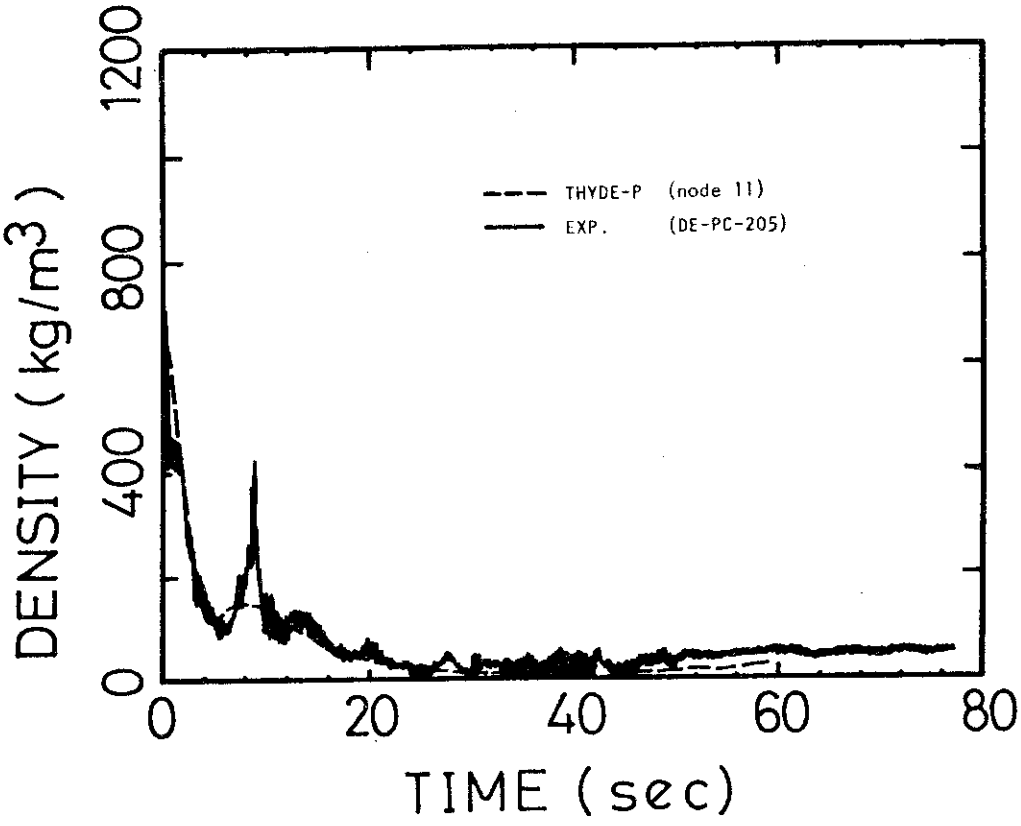

Fig.5.27 Coolant Density at Intact Loop Hot Leg

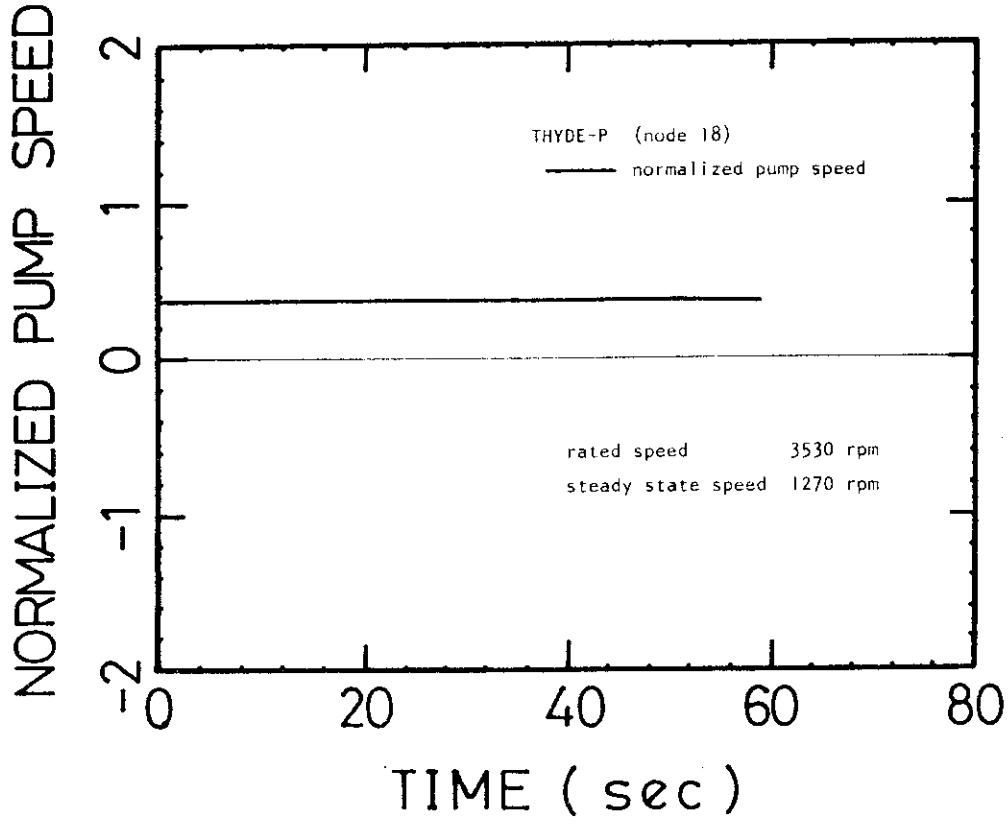

Fig.5.28 Calculated Normalized Pump Speed

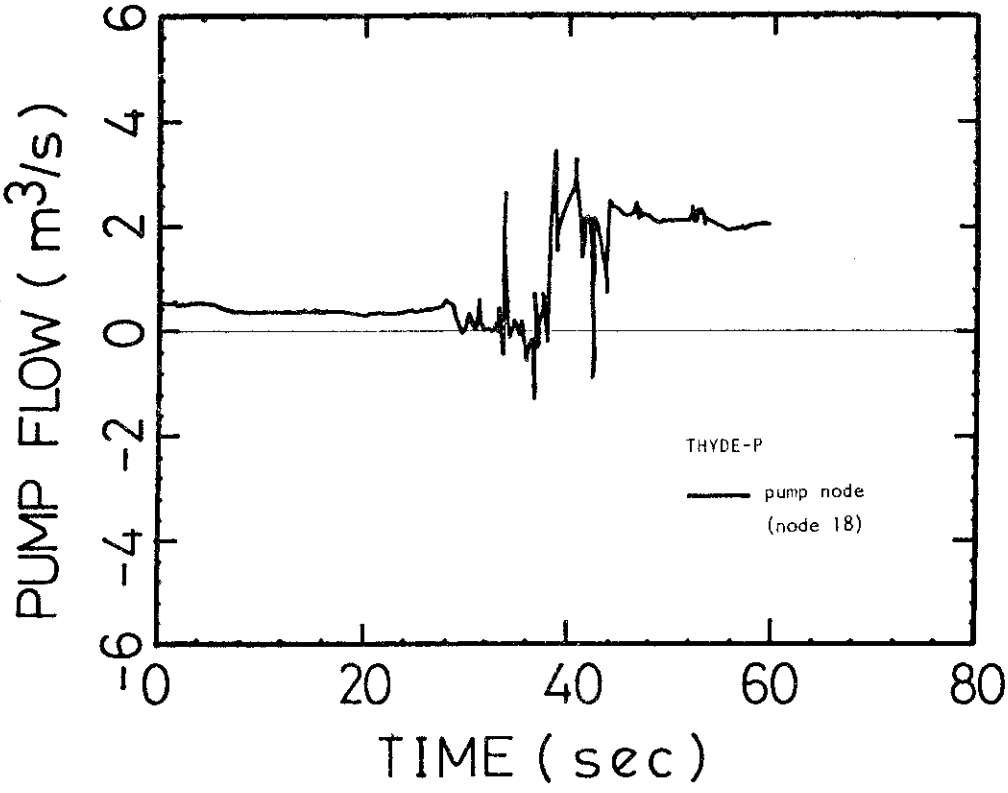

Fig.5.29 Calculated Pump Head

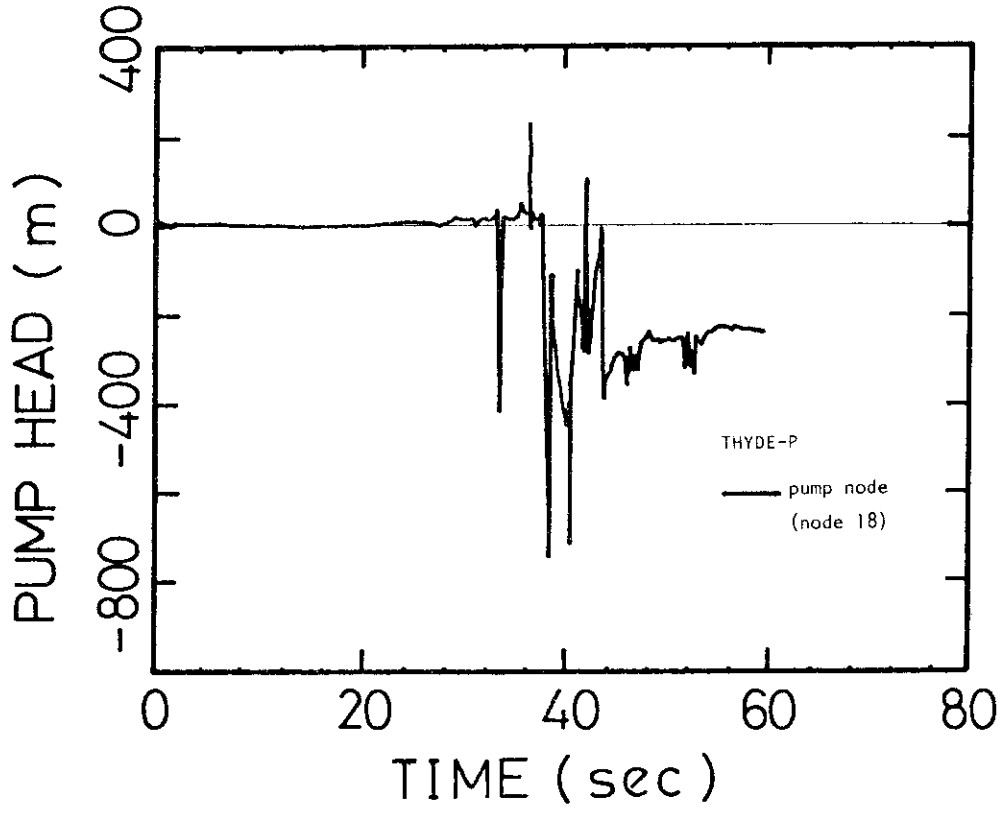

Fig.5.30 Calculated Pump Flow

6. Computing Time and Time Step Width

The CPU time required for the present calculation by a FACOM M-200 computer was about 2 hours. Therefore, the rate of the CPU time to the problem time was about 120. The computer core storage requirment was about 1.2 Mbyte without overlay structure. The maximum time step width allowed by inputs in the present calculation were:

$$t = \begin{cases} 0.001 \text{ sec.} & \text{for} \quad 0.0 \text{ sec.} < t < 0.3 \text{ sec.} \\ 0.004 \text{ sec.} & \text{for} \quad 0.3 \text{ sec.} < t \end{cases}$$

The whole calculation proceeded with the maximum time step width except when rapid transients were calculated.

7. Conclusion

The averall trend of the experiment was well simulated by the present calculation with the THYDE-P code. The rewetting phenomenon at the early stage of the blowdown, which was one of the most characteristic features in LOFT L2-3, was also calculated. Moreover, the calculted core reflood time was in good agreement with the experimental data. Since the present time delay model for density change had very large effects on the core reflood time, it is important to develop a model to evaluate the delay parameter realistically.

The heat transfer correlation package used in the present calculation, which should be considered to be used tentatively, was very simple and therefore refinements must be needed.

Acknowledgement

The author would like to express his thanks to Dr. Y. Asahi, who is the chief auther of the THYDE-P code, for his valuable suggestions to this work. The author's thanks are also due to Mr. K. Sato, Chief of Reactor Safety Code Development Laboratory, and the members of the laboratory for their useful discussions.

6. Computing Time and Time Step Width

The CPU time required for the present calculation by a FACOM M-200 computer was about 2 hours. Therefore, the rate of the CPU time to the problem time was about 120. The computer core storage requirment was about 1.2 Mbyte without overlay structure. The maximum time step width allowed by inputs in the present calculation were:

$$t = \begin{cases} 0.001 \text{ sec.} & \text{for} \quad 0.0 \text{ sec.} < t < 0.3 \text{ sec.} \\ 0.004 \text{ sec.} & \text{for} \quad 0.3 \text{ sec.} < t \end{cases}$$

The whole calculation proceeded with the maximum time step width except when rapid transients were calculated.

7. Conclusion

The averall trend of the experiment was well simulated by the present calculation with the THYDE-P code. The rewetting phenomenon at the early stage of the blowdown, which was one of the most characteristic features in LOFT L2-3, was also calculated. Moreover, the calculted core reflood time was in good agreement with the experimental data. Since the present time delay model for density change had very large effects on the core reflood time, it is important to develop a model to evaluate the delay parameter realistically.

The heat transfer correlation package used in the present calculation, which should be considered to be used tentatively, was very simple and therefore refinements must be needed.

Acknowledgement

The author would like to express his thanks to Dr. Y. Asahi, who is the chief auther of the THYDE-P code, for his valuable suggestions to this work. The author's thanks are also due to Mr. K. Sato, Chief of Reactor Safety Code Development Laboratory, and the members of the laboratory for their useful discussions.

6. Computing Time and Time Step Width

The CPU time required for the present calculation by a FACOM M-200 computer was about 2 hours. Therefore, the rate of the CPU time to the problem time was about 120. The computer core storage requirment was about 1.2 Mbyte without overlay structure. The maximum time step width allowed by inputs in the present calculation were:

$$t = \begin{cases} 0.001 \text{ sec.} & \text{for} \quad 0.0 \text{ sec.} < t < 0.3 \text{ sec.} \\ 0.004 \text{ sec.} & \text{for} \quad 0.3 \text{ sec.} < t \end{cases}$$

The whole calculation proceeded with the maximum time step width except when rapid transients were calculated.

7. Conclusion

The averall trend of the experiment was well simulated by the present calculation with the THYDE-P code. The rewetting phenomenon at the early stage of the blowdown, which was one of the most characteristic features in LOFT L2-3, was also calculated. Moreover, the calculted core reflood time was in good agreement with the experimental data. Since the present time delay model for density change had very large effects on the core reflood time, it is important to develop a model to evaluate the delay parameter realistically.

The heat transfer correlation package used in the present calculation, which should be considered to be used tentatively, was very simple and therefore refinements must be needed.

Acknowledgement

The author would like to express his thanks to Dr. Y. Asahi, who is the chief auther of the THYDE-P code, for his valuable suggestions to this work. The author's thanks are also due to Mr. K. Sato, Chief of Reactor Safety Code Development Laboratory, and the members of the laboratory for their useful discussions.

References

(1) Prassinos, P. G., "Experimental Data Report for LOFT Power Ascension Test L2-3", NUREG/CR-0792 TREE-1326, July 1979.

(2) Reeder, D. L., "LOFT SYSTEM AND TEST DESCRIPTION(5.5 FT CORE1 LOCES)", NUREG/CR-0247 , July 1978.

(3) Asahi, Y., "Description of THYDE-P Code (Preliminary Report of Methods and Models)", JAERI-M 7751, 1978.

(4) Hirano, M and Asahi, Y., "Through Analysis of LOFT L2-2 by THYDE-P Code (I) (Sample Calculation Run 30)", JAERI-M 9535, 1981

(5) Asahi, Y. and Hirano, M., "Verification Study of LOCA Analysis Code THYDE-P (Sample Calculation Run 10)", JAERI-M 8560, 1979.

(6) Zaloudek, F. R., "Steam-Water Critical Flow from High Pressure System", HW-68936, Hanford Works, 1963.

(7) Moody, F. J., "Maximum Floe rate of Single Component, Two-phase Mixture", Heat Trans.-Trans. ASME, 87 n1, pp 134-142, 1965.

(8) Moore, K. V. and Retting, W. H, "RELAP4-A COMPUTER PROGRAM FOR TRANSIENT THERMAL-HYDRAULIC ANALYSIS", ANCR-1127, Dec. 1973.

(9) Dittus, F. W. and Boelter, L. M. K., "Heat Transfer in Automoble Radiators of The Tubular Tube", 2, No. 13, pp 443-461, 1930.

(10) Jens, W. H. and Lottes, P. A., "Analysis of Heat Transfer, Burnout, Pressure Drop and Density Data for High-Pressure Water", ANL-4627, 1951.

(11) Groenevelt, D. C., "An Investigation of Heat Transfer in The Liquid Deficient Regime", Report AECL-3281, Chalk Rever, Ontatio, Dec. 1968.

(12) McEligot, D. M., Ormand, L. W. and Perkins, H. C., J. Trans. Amer. Soc. Mech. Engrs., 88, Series C, pp 239-245, May 1966.

(13) Biasi, L., et. al, "Studies on Burnout : Part 3", Energia Nucleare, pp 550-536, 1967.

(14) McAdams, W. H., "Heat Transmission", 3rd Ed., pp 337, McGrow-Hill, 1954.

(15) McDonough, J. B., Milich, W. and King, E. C., "Partial Film Boiling with Water at 2000 psig in a Round Vertical Tube", MSA Research Corrp., Technical Report 62(NP-6976), 1958.

(16) Zuber, N., Tribus, M. and Westwater, J. W., "The Hydrodynamic Crisis in Pool Boiling of Saturated and Subcooled Liquids", International Developments in Heat Transfer, Part II, pp 230-236, 1961.

(17) Griffith, p., Auedisian, C. T. and Walkush, J. F., "Countercurrent Flow Critical Heat Flux", presented at National Heat Transfer Conference, San Francisco, Aug. 1975.

(18) Thom, J. R. S., et. al, "Boiling in Subcooled Water During Flow Up Heated Tubes or Annuli", Proc. Instn. Mech. Engrs., Vol. 180, Part 3c, pp 226-246, 1966.

(19) Berenson, P. J., "Film-Boiling Heat Transfer from a Horizontal Surface", J. of Heat Transfer, Vol. 83, pp 351-358, Aug. 1961.

Appendix A Input Data List

```
 -- LOFT L2-3 ANALYSIS BY THYDE-P CODE --                80.04.01        00000100
/                                                                        00000200
/  **** DIMENSION DATA ****                                              00000300
BB01                                                                     00000400
  0  0  9  3  17  43  37  9  2  2  1  1  2  6  5  3                      00000500
/                                                                        00000600
/  **** MINOR EDIT DATA ****                                             00000700
BB02                                                                     00000800
PRE-30  PRA-08  PRA-07  GLA-21  GLE-07  GLA-08  GLE-35  GLA-23  GLA-23   00000900
/                                                                        00001000
/  **** TIME STEP CONTROL DATA ****                                      00001100
BB03                                                                     00001200
SB0301                                                                   00001300
    0.2  0.2  100.                                                       00001400
SB0304                                                                   00001500
    30  3  50   0  1.0E-3  1.0E-6  0.3    0.1                           00001600
SB0305                                                                   00001700
    30  3  50   0  4.0E-3  1.0E-6  90.0   0.1                           00001800
SB0308                                                                   00001900
    40  1   1   0  4.0E-3  1.0E-6  2000.0  0.1                          00002000
/                                                                        00002100
/  **** TRIP CONTROLL DATA ****                                          00002200
BB04                                                                     00002300
SB0480                                                                   00002400
  1  0  1  0  1000.0       0.0                                          00002500
SB0481                                                                   00002600
  5 42  1  0     0.002     0.0                                          00002700
SB0482                                                                   00002800
  2 18  1  0  1000.0       0.0                                          00002900
SB0483                                                                   00003000
  2 19  1  0  1000.0       0.0                                          00003100
SB0484                                                                   00003200
  3  0  1  0     0.103     0.0                                          00003300
SB0485                                                                   00003400
  4  1  1  0    14.0       0.0                                          00003500
SB0486                                                                   00003600
  4  2  1  0    29.0       0.0                                          00003700
SB0487                                                                   00003800
 -4  1  1  0  1000.0       0.0                                          00003900
SB0488                                                                   00004000
  -4  2   1  0 1000.0  0.0                                               00004100
SB0489                                                                   00004200
   6  1  -3  1  240.0  0.005                                            00004300
SB0490                                                                   00004400
   6  2  -3  1  250.0  0.0                                              00004500
SB0491                                                                   00004600
   6  3  -3  1  360.0  0.0                                              00004700
SB0492                                                                   00004800
  -6  1   3  1  350.0  0.0                                              00004900
SB0493                                                                   00005000
```

```
----*----1----*----2----*----3----*----4----*----5----*----6----*----7-R--*----8
  -6  2   3  1  305.0  0.0                                                  00005100
SB0494                                                                     00005200
  -6  3   3  1  380.0  0.0                                                  00005300
SB0495                                                                     00005400
   6  2  -2  1  160.0  0.0                                                  00005500
SB0496                                                                     00005600
  -6  2   2  1  190.0  0.0                                                  00005700
/                                                                          00005800
/  **** FLOW AJUST DATA ****                                               00005900
BB05                                                                       00006000
  1      3.1402  347.6                                                     00006100
/                                                                          00006200
/  **** NODE DATA ****                                                     00006300
BB06                                                                       00006400
SB0601                                                                     00006500
 1  1 22 29  0 149.026047915    0.2842     0.0      1.332      0.0         00006600
                                0.4        0.8      0.0        0.0         00006700
SB0602                                                                     00006800
 2  1 29  1  0 148.885342560    0.2842     0.0      0.6965     0.0         00006900
                                0.0        0.0     -1.0       -1.0         00007000
SB0603                                                                     00007100
 3  1  1  2  0 148.885336895    0.1032     0.0      1.517      0.7174      00007200
                               -1.0       -1.0      1.52       1.09        00007300
SB0604                                                                     00007400
 4  1  2  3  0 148.838207175    0.3485     0.0      3.228      2.705       00007500
                                0.0        0.0    189.0      189.0         00007600
SB0605                                                                     00007700
 5  1  3  4  0 148.660515706    0.3485     0.0      3.228     -2.705       00007800
                                0.0        0.0    142.0      198.0         00007900
SB0606                                                                     00008000
 6  1  4  5  0 148.838194913    0.1272     0.0      2.423     -2.0394      00008100
                                0.0        0.0     20.0       20.0         00008200
SB0607                                                                     00008300
 7  1  5  6  0 148.972125842    0.1032     0.0      1.883      1.322       00008400
                                0.0        0.0  -86446.58     0.0         00008500
SB0608                                                                     00008600
 8  1  6  7  0 149.241450804    0.1032     0.0      0.4877     0.0         00008700
                                0.0        0.0     -1.0       -1.0         00008800
SB0609                                                                     00008900
 9  1  7 30  0 149.241451145    0.2842     0.0      0.6965     0.0         00009000
                               -1.0       -1.0      0.0        0.0         00009100
SB0610                                                                     00009200
10  1 30 27  0 149.241451138    0.2842     0.0      0.9510     0.0         00009300
                                0.0        0.0      3.58       3.0         00009400
SB0611                                                                     00009500
11  1 22 23  0 148.64454        0.2842     0.0      2.616      0.0         00009600
                                0.4        0.8      0.0        0.0         00009700
SB0612                                                                     00009800
12  1 23  8  0 148.77914        0.2832     0.0      2.643      0.2432      00009900
                                0.0        0.0     -1.0       -1.0         00010000
SB0613                                                                     00010100
13  1  8  9  0 148.77014        0.9084     0.0      0.5175     0.5175      00010200
                               -1.0       -1.0     -1.0       -1.0         00010300
SB0614                                                                     00010400
14  7  9 10  1 148.71985        0.01021    0.0      2.568      2.483       00010500
                               -1.0       -1.0     -1.0       -1.0         00010600
SB0615                                                                     00010700
15  7 10 11  1 148.49835        0.01021    0.0      2.568     -2.483       00010800
                               -1.0       -1.0     -1.0       -1.0         00010900
```

```
----*----1----*----2----*----3----*----4----*----5----*----6----*----7-R--*----8
                                                                        00011000
SB0616
16  1 11 12  0 148.63618          0.9084     0.0       0.5175    -0.5175  00011100
                                  -1.0       -1.0      -1.0      -1.0     00011200
                                                                        00011300
SB0617
17  1 12 24  0 148.59503          0.2941     0.0       2.426     -1.523   00011400
                                  -1.0       -1.0      0.0        0.0     00011500
                                                                        00011600
SB0618
18  8 24 25  0 148.7532           0.3468     0.0       1.867     1.2807   00011700
                                  0.0        0.0       0.0       0.0      00011800
                                                                        00011900
SB0619
19  8 24 25  0 148.7434           0.3043     0.0       3.111     1.2807   00012000
                                  0.0        0.0       0.0       0.0      00012100
                                                                        00012200
SB0620
20  1 25 26  0 149.4056           0.2757     0.0       1.399     0.0      00012300
                                  0.0        0.0       0.0       0.0      00012400
                                                                        00012500
SB0621
21  1 26 27  0 149.4106           0.2842     0.0       0.5313    0.0      00012600
                                  0.0        0.0       3.58      3.0      00012700
                                                                        00012800
SB0622
22  4 27 13  0 149.2250           0.45190    0.0426    4.256     -4.256   00012900
                                  0.62       0.62      3.5       3.5      00013000
                                                                        00013100
SB0623
23  5 13 28  0 149.4958           1.004      0.0       0.7318    0.0      00013200
                                  0.0        0.0       0.0       0.0      00013300
                                                                        00013400
SB0624
24  1 28 14  0 149.4858           0.4417     0.0       0.4285    0.4285   00013500
                                  0.0        0.0       -1.0      -1.0     00013600
                                                                        00013700
SB0625
25  2 14 15  0 149.3849           1.0        0.0       0.09423   0.09423  00013800
                                  -1.0       -1.0      0.0       0.0      00013900
                                                                        00014000
SB0626
26  2 15 16  1 149.3422           1.0        0.0       0.4191    0.4191   00014100
                                  0.0        0.0       0.0       0.0      00014200
                                                                        00014300
SB0627
27  2 16 17  1 149.2712           1.0        0.0       0.4191    0.4191   00014400
                                  0.0        0.0       0.0       0.0      00014500
                                                                        00014600
SB0628
28  2 17 18  1 149.1979           1.0        0.0       0.4191    0.4191   00014700
                                  0.0        0.0       0.0       0.0      00014800
                                                                        00014900
SB0629
29  2 18 19  1 149.1282           1.0        0.0       0.4191    0.4191   00015000
                                  0.0        0.0       0.0       0.0      00015100
                                                                        00015200
SB0630
30  2 19 20  0 149.0567           1.0        0.0       0.01753   0.01753  00015300
                                  0.0        0.0       -1.0      -1.0     00015400
                                                                        00015500
SB0631
31  1 20 22  0 149.0223           0.5513     0.05486   1.668     1.668    00015600
                                  -1.0       -1.0      0.0       0.0      00015700
                                                                        00015800
SB0632
32  1 28 22  0 149.4858           0.0779     0.0       4.164     4.164    00015900
                                  0.0        0.0       0.0       0.0      00016000
                                                                        00016100
SB0633
33 13 22 37  0   0.1   0.5419    0.0   0.9144   0.9144 0.0  0.0  0.0  0.0 00016200
                                                                        00016300
SB0634
34 13 29 35  0   0.1   0.222     0.0   4.048    0.8620 0.4  0.8  0.0  0.0 00016400
                                                                        00016500
SB0635
35 13 30 36  0   0.1   0.222     0.0   4.840    0.6075 0.4  0.8  0.0  0.0 00016600
                                                                        00016700
SB0636
36 13 23 21  0   4.0   0.043     0.0   4.592    0.4255 0.4  0.8  9.0  9.0 00016800
```

```
----*----1----*----2----*----3----*----4----*----5----*----6----*----7-R--*----8
                                                                        00016900
SB0637
37 13 21 34  0   4.0   0.043    0.0    4.767  0.7678 0.0  0.0  0.0  0.0 00017000
                                                                        00017100
SB0638
38 13 26 31  0  10.0   0.089    0.0    5.5    0.0    0.4  0.8  0.0  0.0 00017200
                                                                        00017300
SB0639
39 13 26 32  0  10.0   0.089    0.0    5.5    0.0    0.4  0.8  0.0  0.0 00017400
                                                                        00017500
SB0640
40 13 26 33  0  10.0   0.089    0.0   58.0    0.0    0.4  0.8  0.0  0.0 00017600
                                                                        00017700
/                                                                       00017800
/  **** JUNCTION DATA ****                                              00017900
BB07                                                                    00018000
     1    1    0.0                                                      00018100
     2    1    0.0                                                      00018200
     3    1    0.0                                                      00018300
     4    1    0.0                                                      00018400
     5    1    0.0                                                      00018500
     6    1    0.0                                                      00018600
     7    1    0.0                                                      00018700
     8    1    0.0                                                      00018800
     9    1    0.0                                                      00018900
    10    1    0.0                                                      00019000
    11    1    0.0                                                      00019100
    12    1    0.0                                                      00019200
    13    1    0.0                                                      00019300
    14    1    0.0                                                      00019400
    15    1    0.0                                                      00019500
    16    1    0.0                                                      00019600
    17    1    0.0                                                      00019700
    18    1    0.0                                                      00019800
    19    1    0.0                                                      00019900
    20    1    0.0                                                      00020000
    21    1    0.0                                                      00020100
    22    4    0.1937                                                   00020200
    23    4    0.04149                                                  00020300
    24    4    0.05040                                                  00020400
    25    4    0.04644                                                  00020500
    26    4    0.08948                                                  00020600
    27    4    0.18                                                     00020700
    28    4    0.064                                                    00020800
    29    4    0.04474                                                  00020900
    30    4    0.04474                                                  00021000
    31    7    0.0                                                      00021100
    32    7    0.0                                                      00021200
    33    5    0.0                                                      00021300
    34    6    0.0                                                      00021400
    35    8    0.0                                                      00021500
    36    8    0.0                                                      00021600
    37    8    0.0                                                      00021700
/                                                                       00021800
/  **** MIXING JUNCTION DATA ****                                       00021900
BB08                                                                    00022000
SB0801                                                                  00022100
    22   3     1   11   33   0   0.001  0.999   0.    0.               00022200
SB0802                                                                  00022300
    23   2    12   36    0   0   1.0    0.0     0.    0.               00022400
SB0803                                                                  00022500
    24   2    18   19    0   0   0.5    0.5     0.    0.               00022600
SB0804                                                                  00022700
    25   1    20    0    0   0   1.0    0.0     0.    0.
```

```
----*----1----*----2----*----3----*----4----*----5----*----6----*----7-R--*----8
SB0805                                                                  00022800
   26   4   21  38  39  40   1.0    0.0     0.    0.                     00022900
SB0806                                                                  00023000
   27   1   22   0   0   0   1.0    0.0     0.    0.                     00023100
SB0807                                                                  00023200
   28   2   24  32   0   0  0.97   0.03     0.    0.                     00023300
SB0808                                                                  00023400
   29   2    2  34   0   0   1.0    0.0     0.    0.                     00023500
SB0809                                                                  00023600
   30   2   10  35   0   0   1.0    0.0     0.    0.                     00023700
/                                                                       00023800
/  **** PUMPED INJECTION DATA ****                                      00023900
BB09                                                                    00024000
SB0901                                                                  00024100
    1   31    24.0                                                      00024200
   10                                                                   00024300
     0.0   0.00     2.0   1.80     4.0   1.47     8.0   1.50           00024400
    28.0   1.60    64.0   1.70    72.0   1.00   120.0   1.00           00024500
   140.0   1.50   200.0   1.50                                          00024600
SB0902                                                                  00024700
    2   32    24.0                                                      00024800
   10                                                                   00024900
     0.0   0.00     3.0   3.50     7.0   4.80    11.0   5.30           00025000
    14.0   5.60    20.0   3.60    27.0   5.20    43.0   6.50           00025100
    59.0   7.00   200.0   7.40                                          00025200
/                                                                       00025300
/  **** PUMP DATA ****                                                  00025400
BB10                                                                    00025500
SB1001                                                                  00025600
 18 1 1 3530. .3155  500.24  108.1  613.73  1269.7  1.4328 .0 .0 1.     00025700
SB1002                                                                  00025800
 19 1 1 3530. .3155  500.24  108.1  613.73  1269.7  1.4328 .0 .0 1.     00025900
/                                                                       00026000
/  **** PUMP DATA TABLE ****                                            00026100
BB11                                                                    00026200
SB1101                                                                  00026300
 1                                                                      00026400
 12                                                                     00026500
 -1.0       2.4722                  -0.80574   2.0474                  00026600
 -0.6096    1.831                   -0.40683   1.624                   00026700
 -0.200171  1.4705                   0.0       1.4036                  00026800
  0.19061   1.3636                   0.38963   1.3186                  00026900
  0.4118    1.3                      0.59396   1.2328                  00027000
  0.7902    1.1336                   1.0       1.0078                  00027100
                                                                        00027200
 12                                                                     00027300
 -1.0                -1.0           -0.80574             -0.6          00027400
 -0.6096             -0.3           -0.40683             -0.05         00027500
 -0.200171            0.13           0.0                  0.25         00027600
  0.19061             0.28           0.38963              0.34         00027700
  0.4118              0.2768         0.59396              0.46         00027800
  0.7902              0.70           1.0                  0.9465       00027900
 17                                                                     00028000
 -1.0       -1.0                    -0.82297  -0.98                     00028100
 -0.63332   -0.95                   -0.45534  -0.90                     00028200
 -0.27109   -0.82                   -0.17716  -0.78                     00028300
 -0.09073   -0.72                    0.0      -0.67                     00028400
  0.091099  -0.60                    0.186509 -0.52                     00028500
  0.271762  -0.42                    0.45582  -0.21                     00028600
  0.574406  -0.02                    0.740576  0.26                     00028700
```

```
----*----1----*----2----*----3----*----4----*----5----*----6----*----7-R--*----8
 0.766619  0.36                    0.871471  0.63                          00028700
 1.0       1.0078                                                        00028800
                                                                         00028900
17                                                                       00029000
-1.0                  2.4722      -0.82297              1.9968           00029100
-0.63332              1.5897      -0.45534              1.3279           00029200
-0.27109              1.1949      -0.17716              1.0605           00029300
-0.09073              1.0156       0.0                  0.934279         00029400
 0.091099             0.9229       0.186509             0.8963           00029500
 0.271762             0.875        0.45582              0.8433           00029600
 0.574406             0.8355       0.740576             0.8466           00029700
 0.766619             0.8469       0.871471             0.8838           00029800
 1.0                  0.9465                                             00029900
14                                                                       00030000
-1.0       1.9843                 -0.80096  1.394                       00030100
-0.60638   1.0975                 -0.40686  0.822                       00030200
-0.30      0.71                   -0.19928  0.6648                      00030300
-0.10      0.61                    0.0      0.6032                      00030400
 0.1930    0.6325                  0.393    0.7369                      00030500
 0.50      0.79                    0.59552  0.8381                      00030600
 0.79782   0.9229                  1.0      0.9672                      00030700
14                                                                       00030800
-1.0                  -1.0        -0.80096              -0.98            00030900
-0.60638              -0.94       -0.40686              -0.91            00031000
-0.30                 -0.90       -0.19928              -0.70            00031100
-0.10                 -0.51        0.0                  -0.45            00031200
 0.1930               -0.37        0.393                -0.26            00031300
 0.50                 -0.01        0.59552               0.06            00031400
 0.79782               0.21        1.0                   0.3569          00031500
17                                                                       00031600
-1.0       -1.0                   -0.82234  -0.98                       00031700
-0.63371   -0.94                  -0.45853  -0.92                       00031800
-0.267023  -0.91                  -0.176107 -0.85                       00031900
-0.089310  -0.80                   0.0      -0.67                       00032000
 0.090643  -0.59                   0.188569 -0.50                       00032100
 0.27347   -0.40                   0.455869 -0.05                       00032200
 0.57448    0.28                   0.73816   0.52                       00032300
 0.76852    0.61                   0.870057  0.74                       00032400
 1.0        0.9672                                                      00032500
17                                                                       00032600
-1.0                  1.9843      -0.82234              1.8308           00032700
-0.63371              1.6824      -0.45853              1.557            00032800
-0.267023             1.4362      -0.176107             1.3879           00032900
-0.089310             1.3481       0.0                  0.23361          00033000
 0.090643             1.1965       0.188569             1.1096           00033100
 0.27347              1.0416       0.455869             0.8958           00033200
 0.57448              0.7807       0.73816              0.6137           00033300
 0.76852              0.5849       0.870057             0.4877           00033400
 1.0                  0.3569                                             00033500
 12                                                                      00033600
 -1.0   -1.15        -0.9  -1.24    -0.6   -2.8        -0.5   -2.9       00033700
 -0.4   -2.7          0.0   0.0      0.12   0.85        0.2    1.1       00033800
 0.5     1.02         0.7   1.0      0.9    0.95        1.0    1.0       00033900
 4                                                                       00034000
 -1.0    0.0          0.0   0.0      0.5   -0.8         1.0   -1.46      00034100
 7                                                                       00034200
 -1.0    0.0          0.0   0.0      0.1   -0.02        0.2    0.0       00034300
  0.3    0.1          0.9   0.78     1.0    1.0                          00034400
 12                                                                      00034500
 -1.0   -1.15        -0.8  -0.5     -0.6   -0.2        -0.4   0.03
```

```
----*----1----*----2----*----3----*----4----*----5----*----6----*----7-R--*----8
  -0.2    0.04         0.0   0.1         0.2    0.15       0.4   0.12       00034600
   0.6    0.05         0.8  -0.5         0.9   -0.9        1.0  -1.46       00034700
                                                                            00034800
 0                                                                          00034900
 0                                                                          00035000
 0                                                                          00035100
 0                                                                          00035200
13                                                                          00035300
 0.0  0.0    0.05 0.0       0.1  0.025       0.15  0.075   0.2  0.18       00035400
 0.3    0.475       0.4     0.625      0.5     0.74         0.6    0.82     00035500
 0.7    0.87        0.8     0.84       0.9     0.72         1.0    0.08     00035600
11                                                                          00035700
 0.0    0.0         0.1     0.0        0.20    0.13         0.3    0.24     00035800
 0.4    0.31        0.5     0.33       0.6     0.3          0.7    0.23     00035900
 0.8    0.16        0.9     0.08       1.0     0.0                          00036000
 6  6                                                                       00036100
 0.0  0.2  0.4  0.6  0.8  1.0                                               00036200
 0.0  0.0  0.0  0.0  0.0  0.0  0.0                                          00036300
 0.2  0.0  3.0650E-5  7.7239E-5  1.3263E-4  1.9460E-4  2.6207E-4           00036400
 0.4  0.0  4.8660E-5  1.2261E-4  2.1053E-4  3.0996E-4  4.1602E-4           00036500
 0.6  0.0  6.3760E-5  1.6066E-4  2.7587E-4  4.0485E-4  5.4514E-4           00036600
 0.8  0.0  7.7239E-5  1.9463E-4  3.3419E-4  4.9044E-4  6.6037E-4           00036700
 1.0  0.0  8.9628E-5  2.2585E-4  3.8780E-4  5.6910E-4  7.6631E-4           00036800
/                                                                           00036900
/  **** ACCUMLATOR DATA ****                                               00037000
BB12                                                                        00037100
SB1201                                                                      00037200
   43   33    1.71   0.96   34.2   41.25      0.9      0.1                 00037300
/                                                                           00037400
/  **** BREAK POINT DATA ****                                               00037500
BB13                                                                        00037600
   6   0.000      0.1   0.8   0.8   0.6   0.8   0.8   0.6                  00037700
   2                                                                        00037800
  0.0      5.0           100.0     5.0                                     00037900
/                                                                           00038000
/  **** PRESSURIZER DATA ****                                               00038100
BB14                                                                        00038200
   41      34       1      0.557     1.7235      0.4        0.4        0.01 00038300
   1.0    1.0     1.0      1.0       1.0         0.0737     0.0737     0.0737 00038400
   0.313 0.313   0.313     1.0       1.0         1.0                       00038500
   2                                                                        00038600
   0.     1.0     1.0      1.0         1000.      1.0        1.0      1.0  00038700
/                                                                           00038800
/  **** STEAM GENERATOR DATA ****                                           00038900
BB15                                                                        00039000
SB1501                                                                      00039100
 42      1845     14     15      2       1                                 00039200
 1.589   4.188   1.0    1.0   0.01905    0.005105  4.469  0.3   213.8  19.5 00039300
 0.000   0.3    60.99                                                       00039400
        -20.0     -8.0                                                    00039500
    0.001     80.   0.5  0.5  0.5                                         00039600
    3                                                                       00039700
    0.0  1.0  1.0  1.0  1.0  1.0  1.0  1.0  1000.0  1.0  1.0  0.0          00039800
/                                                                           00039900
/  **** CORE DATA ****                                                      00040000
BB16                                                                        00040100
   1300     25        30          0          9000.                         00040200
   5.359E-3 6.172E-4    4.647E-3  1.43E-2    0.6     19.52E-6              00040300
   0.0124   2.395E-4    0.0305    1.5897E-3  0.111    1.423E-3             00040400
   0.301    2.869E-3    1.14      8.347E-4   3.01     3.048E-3
```

```
----*----1----*----2----*----3----*----4----*----5----*----6----*----7-R--*----8
  5.0       0.6          4.91E-04  3.41E-06  1.2       1.54E03                 00040500
  0.0     106.605      179.738    137.030     45.427    0.0                     00040600
1.0000E-07  1.00E-07  1.00E-07  1.00E-07  1.000E-07  1.0E-7                    00040700
1.0000E-07  1.00E-07  1.00E-07  1.00E-07  1.000E-07  1.0E-7                    00040800
1.0000E-07  1.00E-07  1.00E-07  1.00E-07  1.000E-07  1.0E-7                    00040900
1.0000E-07  1.00E-07  1.00E-07  1.00E-07  1.000E-07  1.0E-7                    00041000
/                                                                             00041100
/  **** SG RELIEF VALVE DATA ****                                             00041200
BB17                                                                          00041300
                                                                              00041400
    6                                                                         00041500
  0.  0.  0.1  -14.   0.18  -32.  0.34  -62.  0.5  -94.  0.58  -179.          00041600
    4                                                                         00041700
 50. -0.00030  380.  -0.00022  1200. -0.00015  2280.  -0.00008                00041800
    9                                                                         00041900
  0.0  0.0  0.2   -0.2  0.4   -0.4    0.6   -1.4   0.8    -2.6                00042000
  1.0 -5.6  1.2  -12.6  1.4  -15.4  200.0  -15.6                              00042100
/                                                                             00042200
/   ****                      ****                                            00042300
BB18                                                                          00042400
    1.54E03     0.775E-04    2.29E04                                          00042500
/                                                                             00042600
/  **** FUEL GAP DATA ****                                                    00042700
BB19                                                                          00042800
 5.7E-4  0.0     5.493E-6  0.0    0.0                                         00042900
 0.0     0.0     0.9       0.75   0.0                                         00043000
 0.887   0.0355  0.0063    0.0    0.0712                                      00043100
 0.0     0.0                                                                  00043200
/                                                                             00043300
/  ****                     ****                                            00043400
BB21                                                                          00043500
2  2  5.00E7    6.96E-08  2.87E4   2.86E-03  1.15E0  1.528E0                 00043600
      1.49E-07  2.0E-08  1.25E-16  1.85E-01  8.0E09  3.3E-03                 00043700
/                                                                             00043800
/  **** OTHER DATA ****                                                       00043900
BB22                                                                          00044000
   0. 1.4  1.4  0.                                                            00044100
BEND                                                                          00044200
6                                                                             00044300
  0  0     0  0  0  0.                                                       00044400
  0. 1.E-5 0. 0. 0. 0.                                                       00044500
END
```

Appendix B Nomenclature

c_n	Quantity defined in Subsec. 3.4, s
G	Mass flux, kg/m^2s
G_{min}	Mass flux defined in Subsec 3.1, kg/m^2s
h	Coolant enthalpy, kcal/kg
h_{gs}	Saturated steam enthalpy, kcal/kg
h_{fs}	Saturated fluid enthalpy, kcal/kg
Re	Reynolds number, -
$T_{coolant}$	Coolant temperature, °c
T_{wall}	Wall temperature, °c
T_{sat}	Coolant saturation temperature, °c
ΔT_s	Wall superheat, °c
ΔT_{min}	Minimum film boiling wall superheat, °c
x	Coolant quality, -
x_c	Coolant quality defined in Subsec. 3.2, -
α	Equilibrium void fraction, -
α^*	Non-equilibrium void fraction, -
ρ	Equilibrium node average density, kg/m^3
ρ^*	Non-equilibrium node average density, kg/m^3
ρ_{gs}	Saturated steam density, kg/m^3
ρ_{fs}	Saturated fluid density, kg/m^3
τ_D	Delay parameter, s
ϕ	Heat flux, $kcal/m^2s$
ϕ_c	Heat flux defined in Subsec. 3.2, $kcal/m^2s$
ϕ_{CHF}	Critical heat flux, $kcal/m^2s$
ϕ_{4-1}	Heat flux calculated by using heat transfer mode 4.1, $kcal/m^2s$
ϕ_{4-2}	Heat flux calculated by using heat transfer mode 4.2, $kcal/m^2s$